QRPA for deformed and odd nuclei study and systematic calculations

S. Péru,

CEA, DAM, DIF, France

1. QRPA : standard expressions and uses
2. QRPA for deformed nuclei
3. Some systematic QRPA calculations
4. QRPA for odd nuclei
5. QRPA and its unusual application

Short Reminder

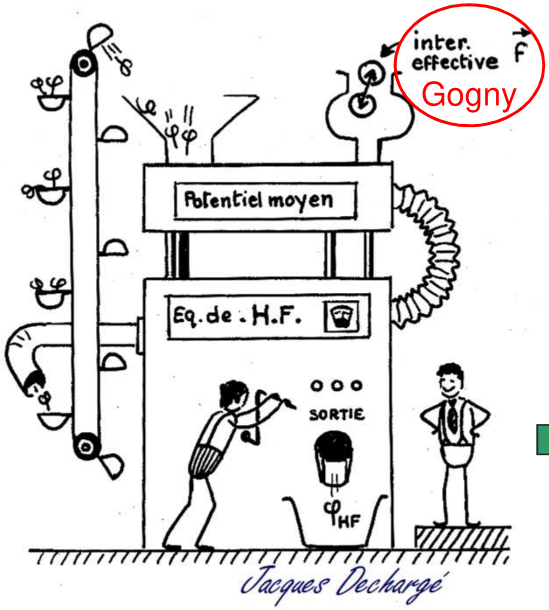

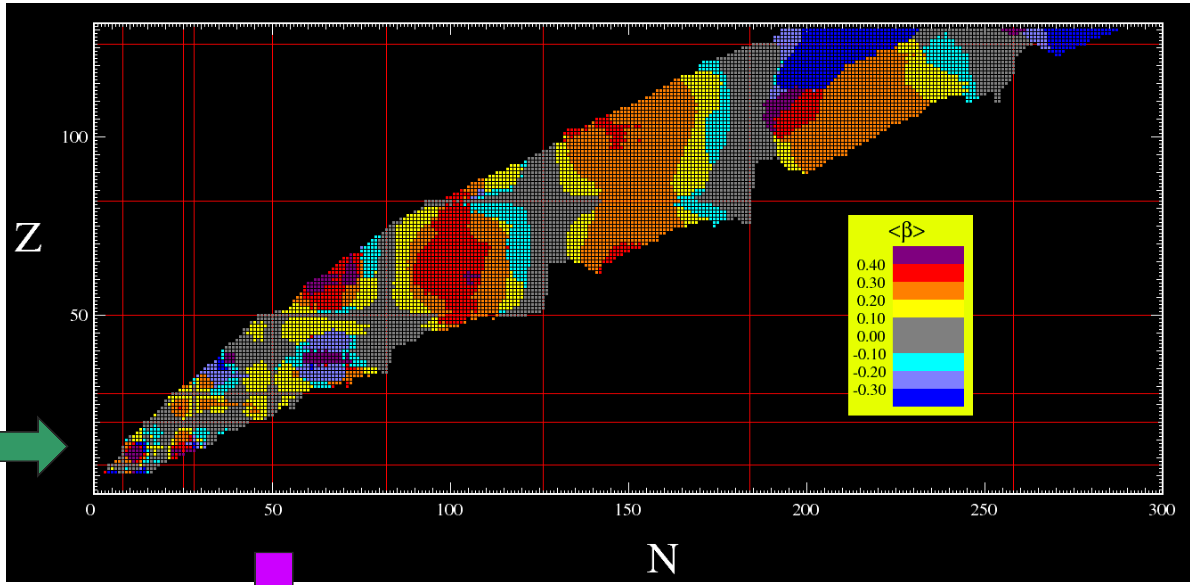

Static mean field (HFB)
for Ground State Properties :

- Masses
- Deformation
- (Single particle levels)

Amedee database :
http://www-phynu.cea.fr/HFB-Gogny_eng.htm
*S. Hilaire & M. Girod, EPJ **A33** (2007) 237*

Beyond static mean field approximation
(5DCH, GCM, MPMH, TDHFB … or QRPA)
for description of Excited State Properties

- Low-energy collective levels
- Giant Resonances

1. QRPA : standard expressions and uses

What is the standard QRPA approach ?

The (Q)RPA methods describe nuclear excited states for all multipoles and both parities, whatever the intrinsic deformation of the ground state.

Quadrupole, octupole and higher multipolarities can be obtained even on top of spherical shapes.

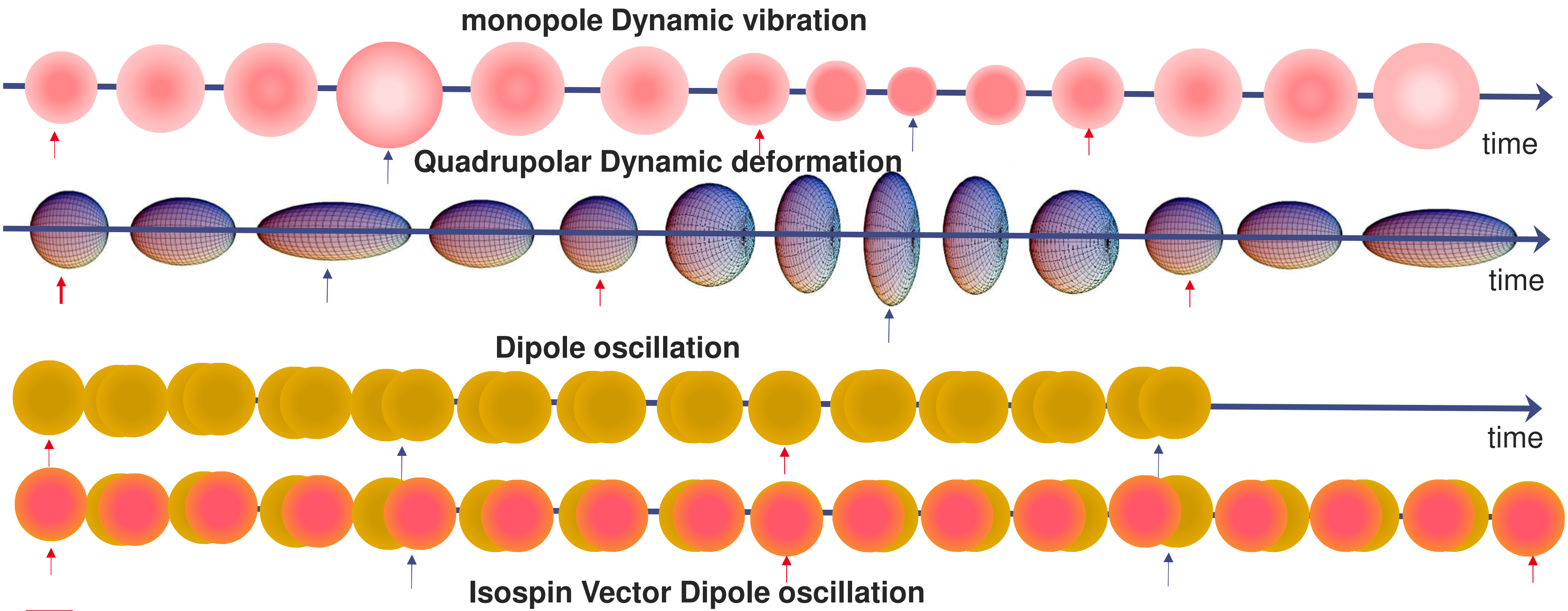

What is the standard QRPA approach ?

The (Q)RPA methods describe nuclear excited states for all multipoles and both parities whatever the intrinsic deformation of the ground state.

No rotational motion included even for deformed nuclei !

Main approximation:

Linear response, i.e. harmonic potential approximation

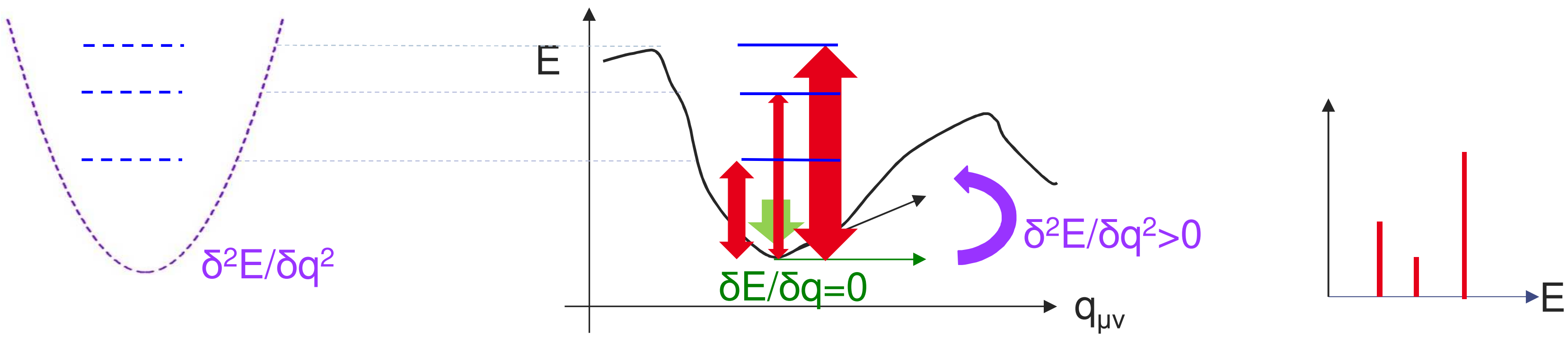

And the result looks like this

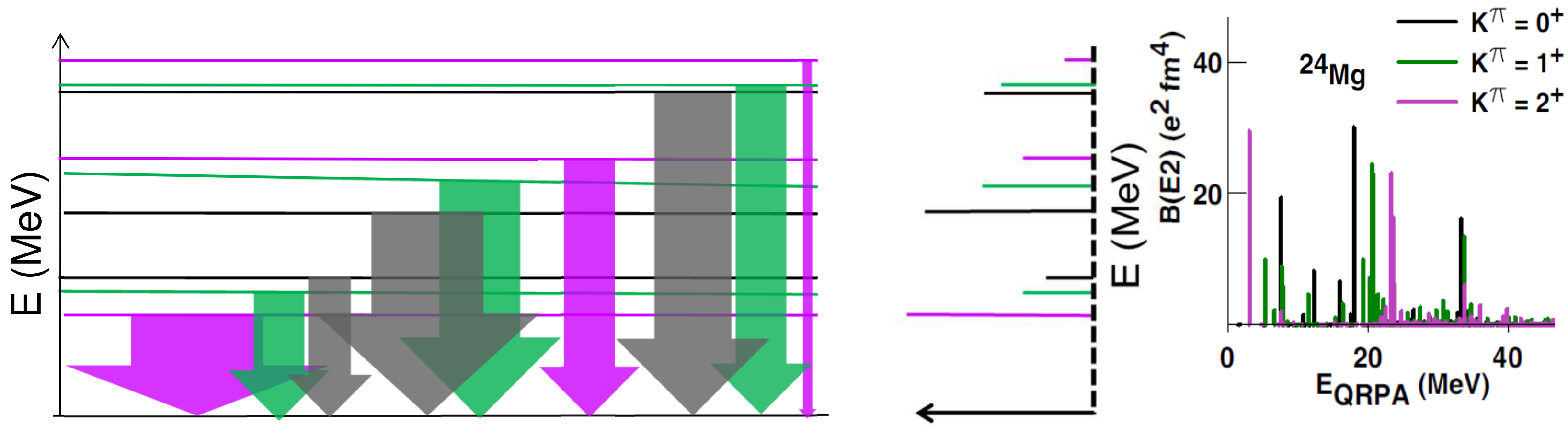

Monopole in Ni isotopes

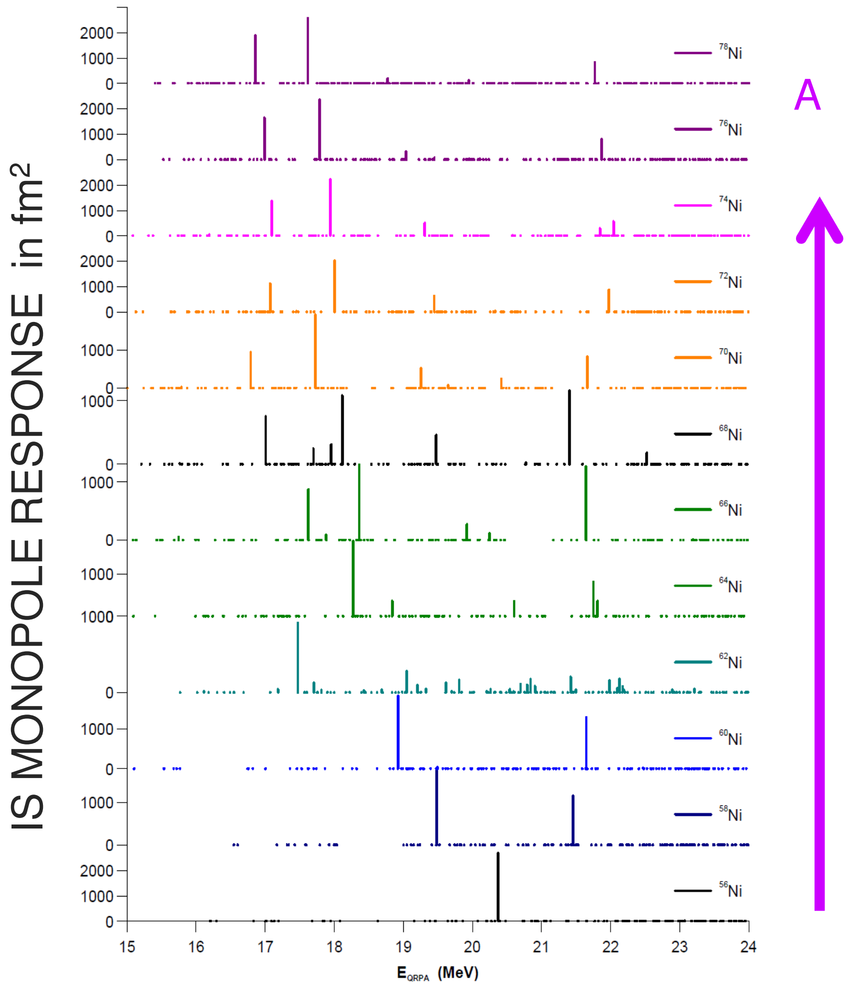

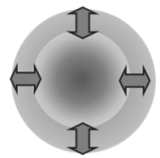

With A ↑ split in two components ↑

Low energy part ↓ with $A^{-1/3}$

RPA approaches describe collective and individual states

Dipole response for Neon isotopes and N=16 isotones

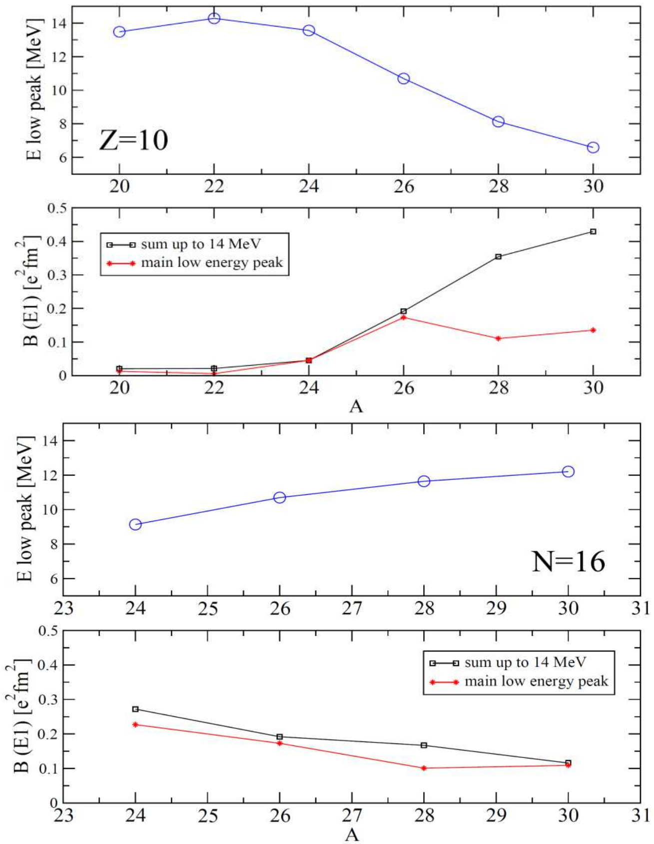

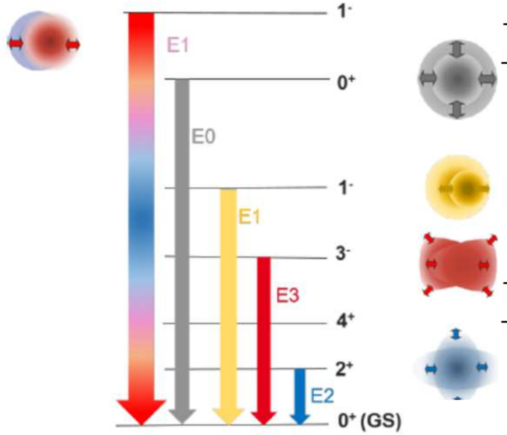

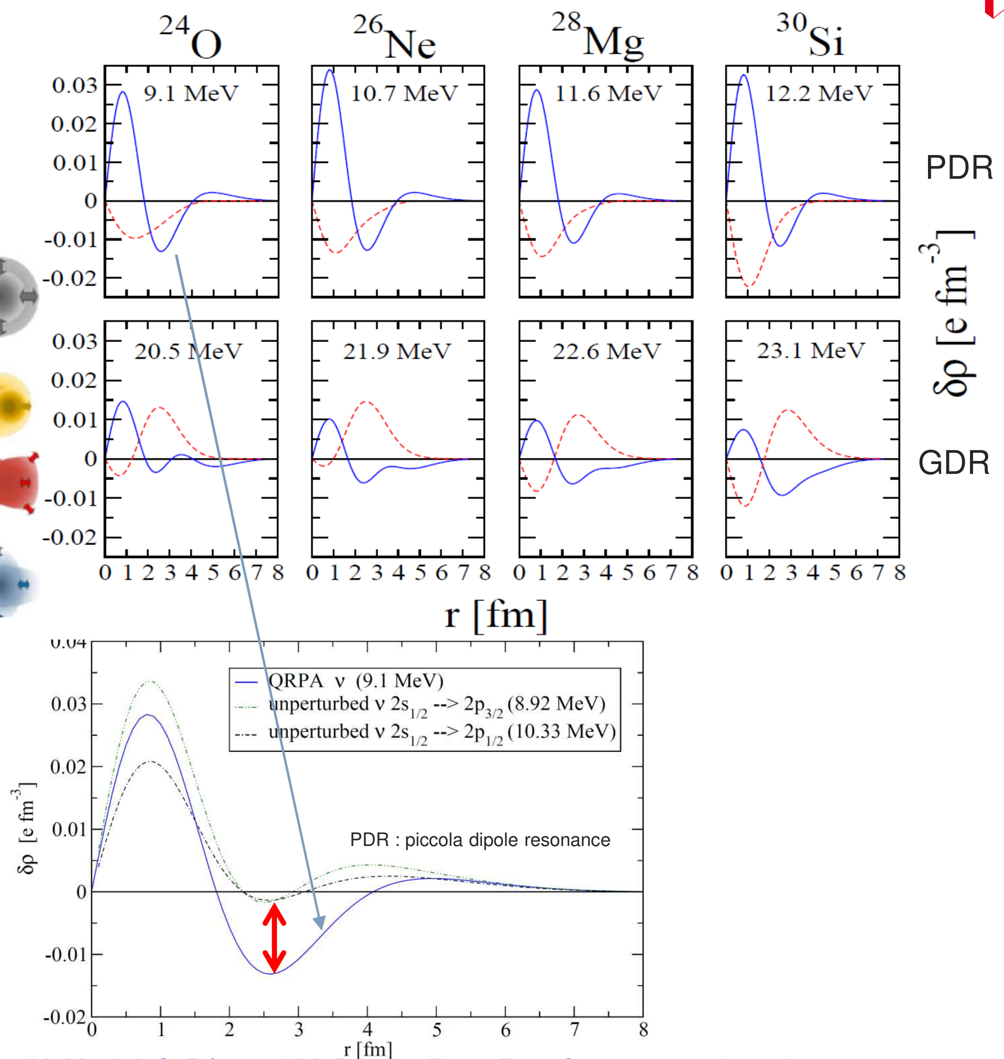

Increasing |N-Z| number :

- **Low energy dipole resonances shift to low energies**
- **Increasing of fragmentation and collectivity**

M. Martini, S. Péru and M. Dupuis, Phys. Rev. C **83**, 034309 (2011)

(Q)RPA approaches describe all multipolarities and all parities

A. Corsi et al PLB 743 (2015) 451-455

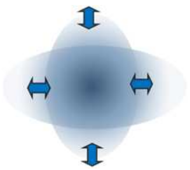

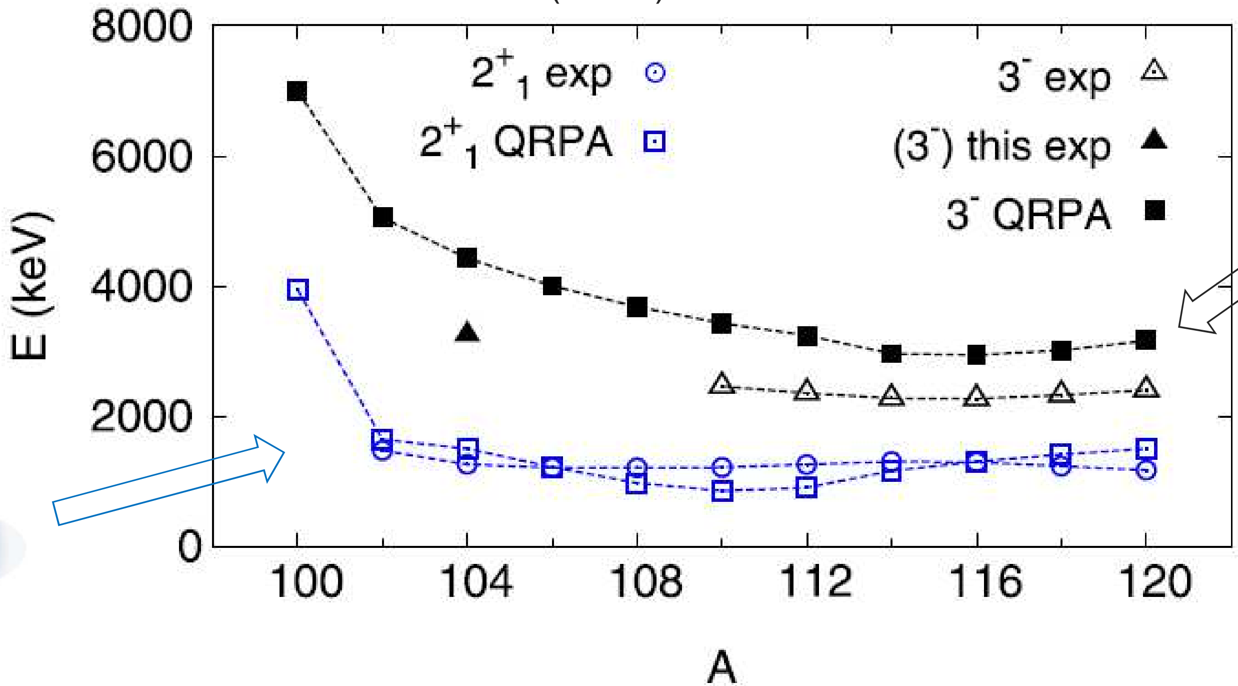

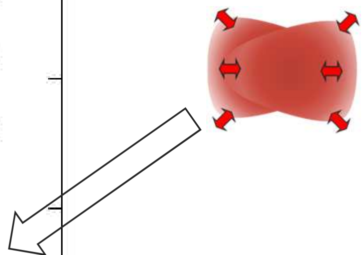

Fig. 3. (Color online.) Systematics of 2^+ and 3^- excitation energies in tin isotopes from experiment and HFB + QRPA calculations using the Gogny D1M interaction.

HFB formalism

$$F\left(\rho,\kappa\right)=\sum_{\alpha\beta} t_{\alpha\beta}\rho_{\beta\alpha}+\frac{1}{2}\sum_{\alpha\beta\gamma\delta}\langle\alpha\beta|\mathcal{V}(\rho)|\widetilde{\gamma\delta}\rangle\rho_{\gamma\alpha}\rho_{\delta}+\frac{1}{4}\sum_{\alpha\beta\gamma\delta}\langle\alpha\beta|\mathcal{V}(\rho)|\widetilde{\gamma\delta}\rangle\kappa^{*}_{\beta\alpha}\kappa_{\gamma\delta}$$

$$\delta F=\sum_{\alpha\beta}\frac{\partial F}{\partial\rho_{\beta\alpha}}\delta\rho_{\alpha\beta}+\frac{1}{2}\sum_{\alpha\beta}\left(\frac{\partial F}{\partial\kappa_{\beta\alpha}}\delta\kappa_{\alpha\beta}+\frac{\partial F}{\partial\kappa^{*}_{\beta\alpha}}\delta\kappa^{*}_{\alpha\beta}\right)$$

$$H_B=\begin{pmatrix} e & \Delta \\ -\Delta^{*} & -e^{*}\end{pmatrix} \qquad e_{\alpha\beta}=\frac{\partial F}{\partial\rho_{\beta\alpha}} \qquad \Delta_{\alpha\beta}=\frac{\partial F}{\partial\kappa^{*}_{\alpha\beta}}$$

$$\mathcal{R}=\begin{pmatrix} \rho & \kappa \\ -\kappa^{*} & (1-\rho^{*})\end{pmatrix}$$

$$[H_B,\mathcal{R}]=0$$

(Q)RPA formalism 1/3

$$F(\rho,\kappa) = \sum_{\alpha\beta} t_{\alpha\beta}\rho_{\beta\alpha} + \frac{1}{2}\sum_{\alpha\beta\gamma\delta} \langle\alpha\beta|\mathcal{V}(\rho)|\widetilde{\gamma\delta}\rangle \rho_{\gamma\alpha}\rho_{\delta\beta} + \frac{1}{4}\sum_{\alpha\beta\gamma\delta} \langle\alpha\beta|\mathcal{V}(\rho)|\widetilde{\gamma\delta}\rangle \kappa^{*}_{\beta\alpha}\kappa_{\gamma\delta}$$

$$\delta F_2 = \frac{1}{2}\sum_{\alpha\beta}\left[\delta\rho_{\alpha\beta}\sum_{\gamma\delta}\left(V^{CM}_{\beta\alpha,\delta\gamma}\delta\rho_{\gamma\delta} + V^{M}_{\beta\alpha,\delta\gamma}\delta\kappa_{\gamma}\right. + \delta\kappa_{\alpha\beta}\sum_{\gamma\delta}\left(V^{M*}_{\beta\alpha,\delta\gamma}\delta\rho_{\gamma\delta} + V^{P}_{\beta\alpha,\delta\gamma}\delta\kappa_{\gamma\delta}\right)\right]$$

$$V^{CM}_{\beta\alpha,\gamma\delta} = \frac{1+\delta_{\alpha\beta}}{2}\frac{1+\delta_{\gamma\delta}}{2}\frac{\partial^2 F}{\partial\rho_{\alpha\beta}\partial\rho_{\gamma\delta}}$$

$$V^{M}_{\beta\alpha,\gamma\delta} = \frac{1+\delta_{\alpha\beta}}{2}\frac{1+\delta_{\gamma\delta}}{2}\frac{\partial^2 F}{\partial\rho_{\alpha\beta}\partial\kappa_{\gamma\delta}}$$

$$V^{M*}_{\beta\alpha,\gamma\delta} = \frac{1+\delta_{\alpha\beta}}{2}\frac{1+\delta_{\gamma\delta}}{2}\frac{\partial^2 F}{\partial\partial\kappa_{\alpha\beta}\rho_{\gamma\delta}}$$

$$V^{P}_{\beta\alpha,\gamma\delta} = \frac{1+\delta_{\alpha\beta}}{2}\frac{1+\delta_{\gamma\delta}}{2}\frac{\partial^2 F}{\partial\kappa_{\alpha\beta}\partial\kappa_{\gamma\delta}}$$

$$A_{ph,p'h'} = (\epsilon_p - \epsilon_h)\delta_{pp'}\delta_{hh'} + \frac{\partial^2 F}{\partial\rho_{hp}\partial\rho_{p'h'}}$$

$$B_{ph,p'h'} = \frac{\partial^2 F}{\partial\rho_{hp}\partial\rho_{h'p'}}$$

$$\begin{pmatrix} A & B \\ B & A \end{pmatrix}\begin{pmatrix} X_n \\ Y_n \end{pmatrix} = \omega_n \begin{pmatrix} X_n \\ -Y_n \end{pmatrix}$$

(Q)RPA formalism 2/3

$$
\begin{aligned}
V^{CM}_{\alpha\beta,\gamma\delta} =& \frac{1+\delta_{\alpha\beta}}{2}\frac{1+\delta_{\gamma\delta}}{2}\frac{\partial^2 F}{\partial\rho_{\beta\alpha}\partial\rho_{\gamma\delta}} \\
=& \langle\alpha\gamma|\mathcal{V}|\widetilde{\beta\delta}\rangle \\
&+\sum_{\gamma'\delta'}\langle\alpha\gamma'|\frac{\partial\mathcal{V}}{\partial\rho_{\delta\gamma}}|\widetilde{\beta\delta'}\rangle\rho_{\delta'\gamma'} \\
&+\sum_{\gamma'\delta'}\langle\gamma\gamma'|\frac{\partial\mathcal{V}}{\partial\rho_{\alpha\beta}}|\widetilde{\delta\delta'}\rangle\rho_{\delta'\gamma'} \\
&+\frac{1}{2}\sum_{\gamma'\delta'\gamma''\delta''}\langle\gamma'\gamma''|\frac{\partial^2\mathcal{V}}{\partial\rho_{\delta\gamma}\partial\rho_{\alpha\beta}}|\widetilde{\delta'\delta''}\rangle\rho_{\delta'\gamma'}\rho_{\delta''\gamma''} \\
&+\frac{1}{2}\sum_{\gamma'\delta'\gamma''\delta''}\langle\gamma'\overline{\gamma''}|\frac{\partial^2\mathcal{V}}{\partial\rho_{\delta\gamma}\partial\rho_{\alpha\beta}}|\widetilde{\delta'\overline{\delta''}}\rangle\kappa_{\gamma''\gamma'}\kappa_{\delta'\delta''}. \quad (46)
\end{aligned}
$$

$$
\begin{aligned}
&\sum_{\gamma'\delta'}\langle\alpha\gamma'|\frac{\partial\mathcal{V}}{\partial\rho_{\gamma\delta}}|\widetilde{\beta\delta'}\rangle\rho_{\delta'\gamma'} = \\
&\delta_{\sigma_\alpha\sigma_\beta}\delta_{\sigma_\gamma\sigma_\delta}\delta_{\tau_\alpha\tau_\beta}\delta_{\tau_\gamma\tau_\delta}t_0\alpha_0 \\
&\cdot\left\langle\alpha\gamma\middle|\delta(r_1-r_2)\rho^{\alpha_0-1}\left(\left(1+\frac{x_0}{2}\right)\rho\right.\right. \\
&\left.\left.-\left(x_0+\frac{1}{2}\right)\rho^{\tau_\alpha}\right)\middle|\beta\delta\right\rangle
\end{aligned}
$$

$$
\begin{aligned}
&\sum_{\gamma'\delta'\gamma''\delta''}\langle\gamma'\gamma''|\frac{\partial^2\mathcal{V}}{\partial\rho_{\alpha\beta}\partial\rho_{\gamma\delta}}|\widetilde{\delta'\delta''}\rangle\rho_{\delta'\gamma'}\rho_{\delta''\gamma''} = \\
&\delta_{\sigma_\alpha\sigma_\beta}\delta_{\sigma_\gamma\sigma_\delta}\delta_{\tau_\alpha\tau_\beta}\delta_{\tau_\gamma\tau_\delta}t_0\alpha_0\left(\alpha_0-1\right) \\
&\cdot\left\langle\alpha\gamma\middle|\delta(r_1-r_2)\rho^{\alpha_0-2}\left(\left(1+\frac{x_0}{2}\right)\rho^2\right.\right. \\
&\left.\left.-\left(x_0+\frac{1}{2}\right)\sum_\tau\rho^{\tau_\alpha\,2}\right)\middle|\beta\delta\right\rangle. \quad (49)
\end{aligned}
$$

$$
\begin{aligned}
\mathbf{A}_{ij,kl} =& (\epsilon_i+\epsilon_j)\delta_{ik}\delta_{jl} \\
&+\frac{1}{2}\sum_{\alpha\beta\gamma\delta}(1+\delta_{\alpha\beta})(1+\delta_{\gamma\delta})\langle\alpha\beta|\mathcal{V}|\widetilde{\gamma\delta}\rangle \\
&\Big(\tilde{U}_{i\alpha}\tilde{V}_{j\gamma}U_{\delta k}V_{\beta l}-\tilde{U}_{i\alpha}\tilde{V}_{j\gamma}V_{\beta k}U_{\delta l} \\
&-\tilde{V}_{i\gamma}\tilde{U}_{j\alpha}U_{\delta k}V_{\beta l}+\tilde{V}_{i\gamma}\tilde{U}_{j\alpha}V_{\beta k}U_{\delta l} \\
&+\tilde{U}_{i\alpha}\tilde{U}_{j\beta}U_{\gamma k}U_{\delta l}+V_{\gamma i}V_{\delta j}\tilde{V}_{k\alpha}\tilde{V}_{l\beta}\Big), \quad (50)
\end{aligned}
$$

$$
\begin{aligned}
\mathbf{B}_{ij,kl} =& \frac{1}{2}\sum_{\alpha\beta\gamma\delta}(1+\delta_{\alpha\beta})(1+\delta_{\gamma\delta})\langle\alpha\beta|\mathcal{V}|\widetilde{\gamma\delta}\rangle \\
&\Big(\tilde{U}_{i\alpha}\tilde{V}_{j\gamma}V_{\delta k}U_{\beta l}-\tilde{U}_{i\alpha}\tilde{V}_{j\gamma}U_{\beta k}V_{\delta l} \\
&-\tilde{V}_{i\gamma}\tilde{U}_{j\alpha}V_{\delta k}U_{\beta l}+\tilde{V}_{i\gamma}\tilde{U}_{j\alpha}U_{\beta k}V_{\delta l} \\
&+\tilde{U}_{i\alpha}\tilde{U}_{j\beta}V_{\delta k}V_{\gamma l}+\tilde{V}_{i\delta}\tilde{V}_{j\gamma}U_{\alpha k}U_{\beta l}\Big), \quad (51)
\end{aligned}
$$

S. P, M. Martini, EPJA (2014) 50:88

(Q)RPA Formalism 3/3

$$H|\nu\rangle = E_\nu|\nu\rangle \qquad Q_\nu^\dagger|0\rangle = |\nu\rangle \qquad Q_\nu|0\rangle = 0$$

Particle-hole excitations: RPA

$$Q_\nu^\dagger = \sum_{ph} X_{ph}^{\nu}\, a_p^\dagger a_h - Y_{ph}^{\nu}\, a_h^\dagger a_p$$

2 quasi-particles excitations: QRPA

$$Q_\nu^+ = \sum_{ij} X_{ij}^{\nu} \eta_i^+ \eta_j^+ + Y_{ij}^{\nu} \eta_j \eta_i \qquad \eta_i^+ = \sum_\alpha u_{i\alpha} a_\alpha^+ - v_{i\alpha} a_\alpha$$

$$\begin{pmatrix} A & B \\ B^* & A^* \end{pmatrix} \begin{pmatrix} X^\nu \\ Y^\nu \end{pmatrix} = \omega_\nu \begin{pmatrix} X^\nu \\ -Y^\nu \end{pmatrix}$$

Hartree-Fock Bogoliubov: ε, u, v ⟶ Ground state properties

QRPA: ω, X, Y ⟶ Excited states properties

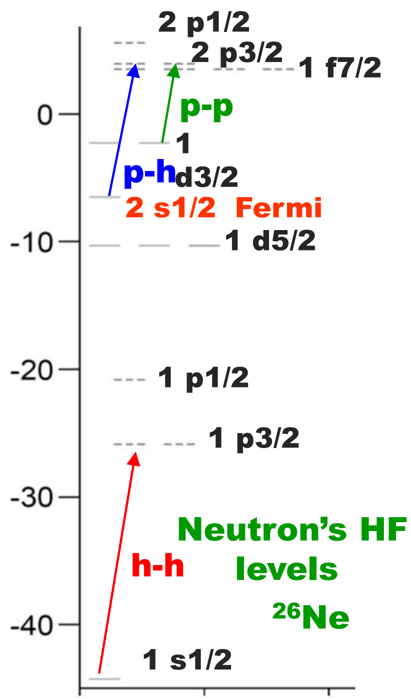

Role of the consistence between HF and RPA matrices

RPA in spherical symmetry

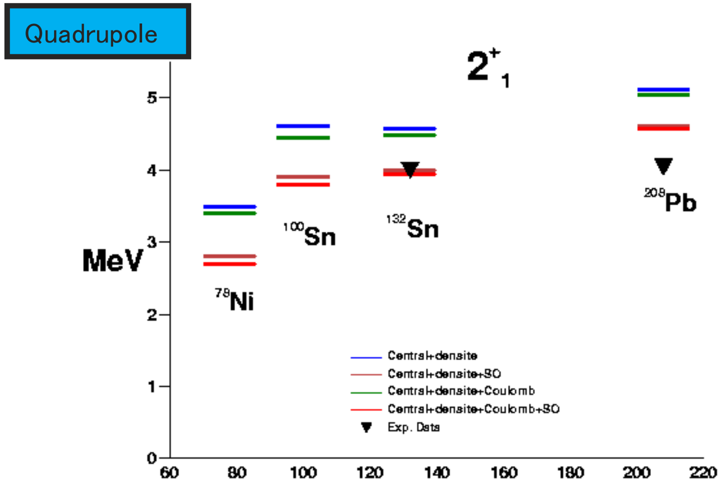

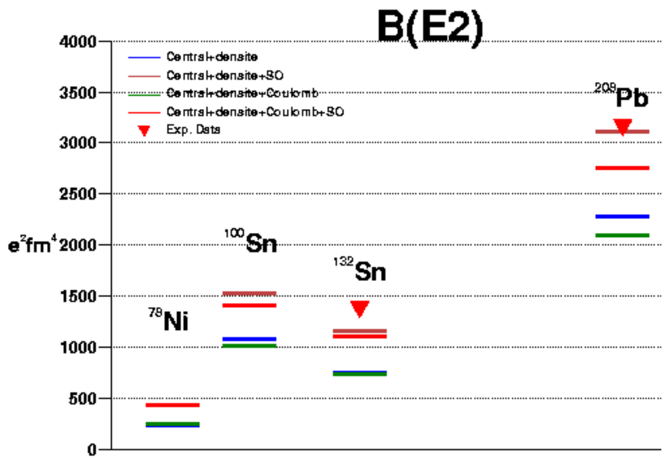

S. Péru, J.F. Berger, and P.F. Bortignon, Eur. Phys. Jour. A **26**, 25-32 (2005)

$$V(1,2) = \sum_{j=1,2} e^{-\frac{(\vec{r}_1-\vec{r}_2)^2}{\mu_j^2}} \left(W_j + B_j P_\sigma - H_j P_\tau - M_j P_\sigma P_\tau\right)$$ central **finite range**

$$+t_0\left(1+x_0 P_\sigma\right)\delta\left(\vec{r}_1-\vec{r}_2\right)\left[\rho\left(\frac{\vec{r}_1+\vec{r}_2}{2}\right)\right]^\alpha$$ density dependent

$$+i W_{ls} \overleftarrow{\nabla}_{12}\delta\left(\vec{r}_1-\vec{r}_2\right)\times\overrightarrow{\nabla}_{12}.\left(\vec{\sigma}_1+\vec{\sigma}_2\right)$$ spin-orbit

Impact of cutoff energy in 2qp excitation basis

Sn isotopes

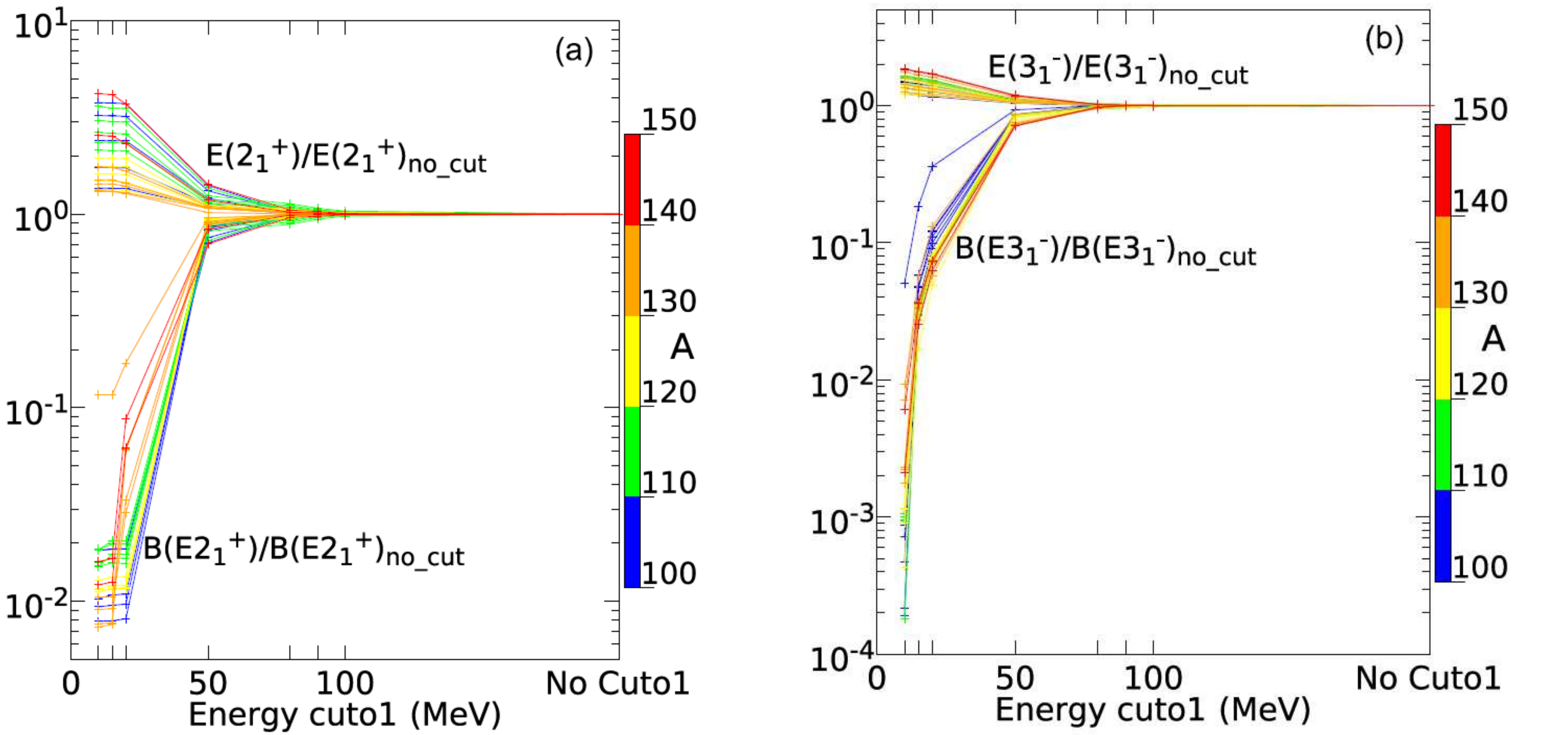

F. Lechaftois, I. Deloncle, S. P, PRC92,034315 (2015)

Impact of frozen core

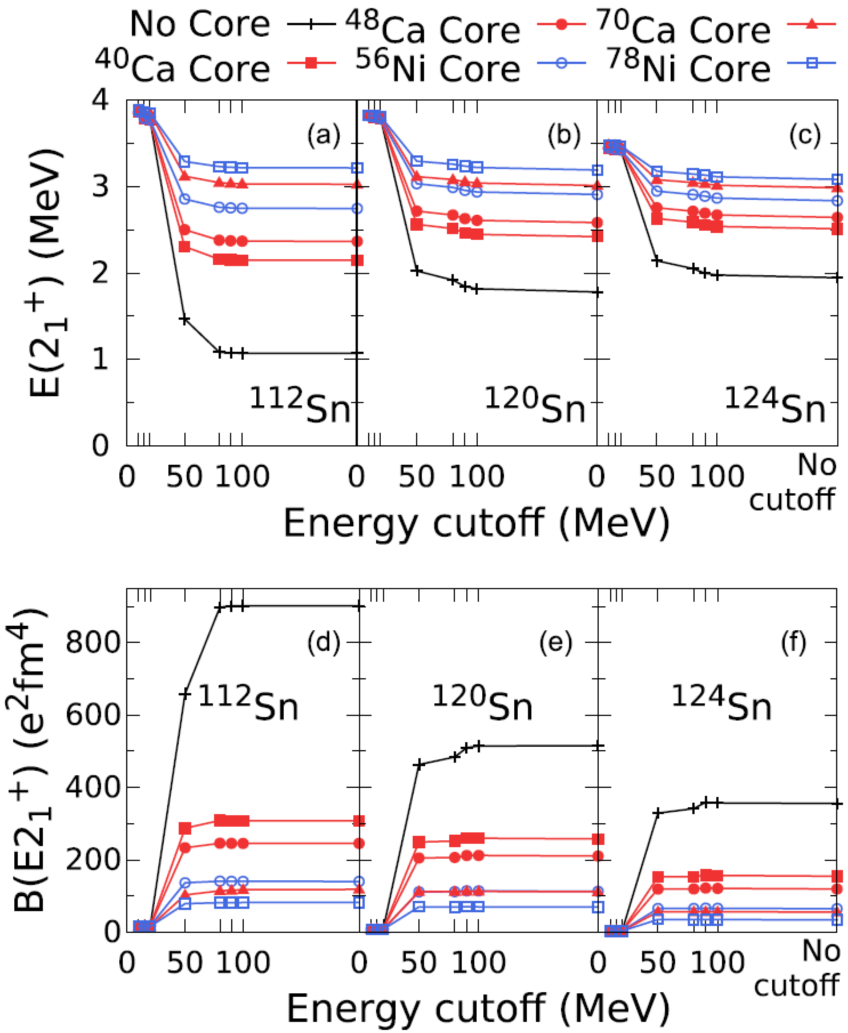

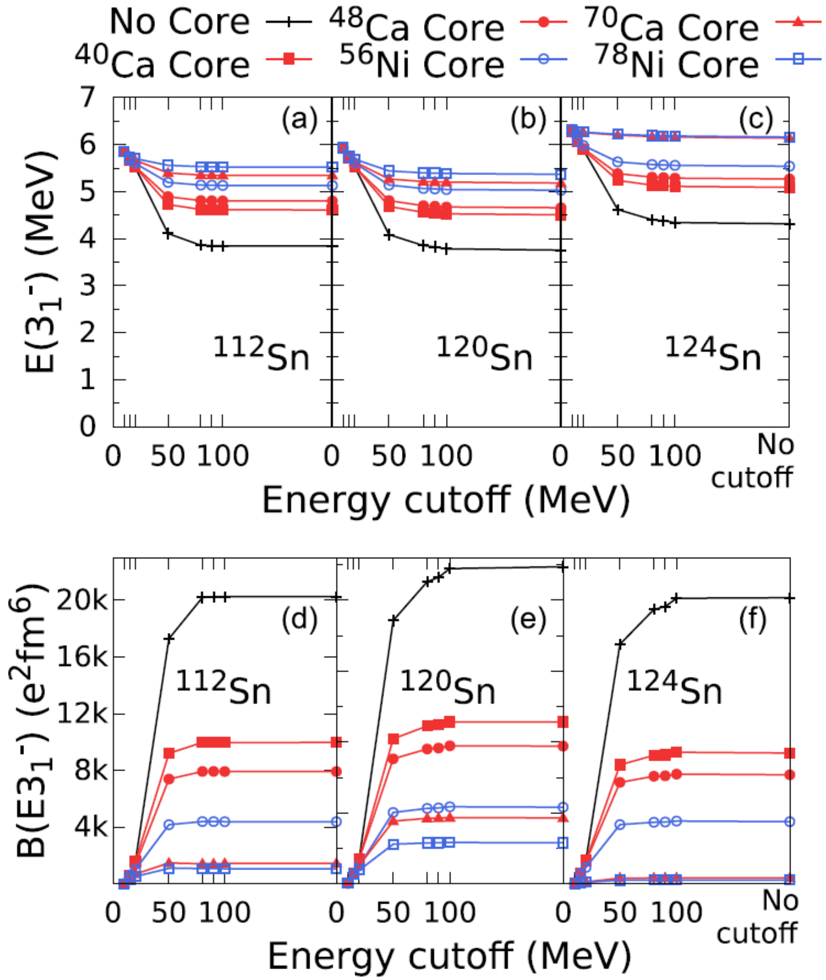

F. Lechaftois, I. Deloncle, S.P., PRC92,034315 (2015)

Spurious states « treatment »

PHYSICAL REVIEW C **83**, 014314 (2011)

Giant resonances in ^{238}U within the quasiparticle random-phase approximation with the Gogny force

S. Péru,[1,*] G. Gosselin,[1] M. Martini,[1] M. Dupuis,[1] S. Hilaire,[1] and J.-C. Devaux[2]

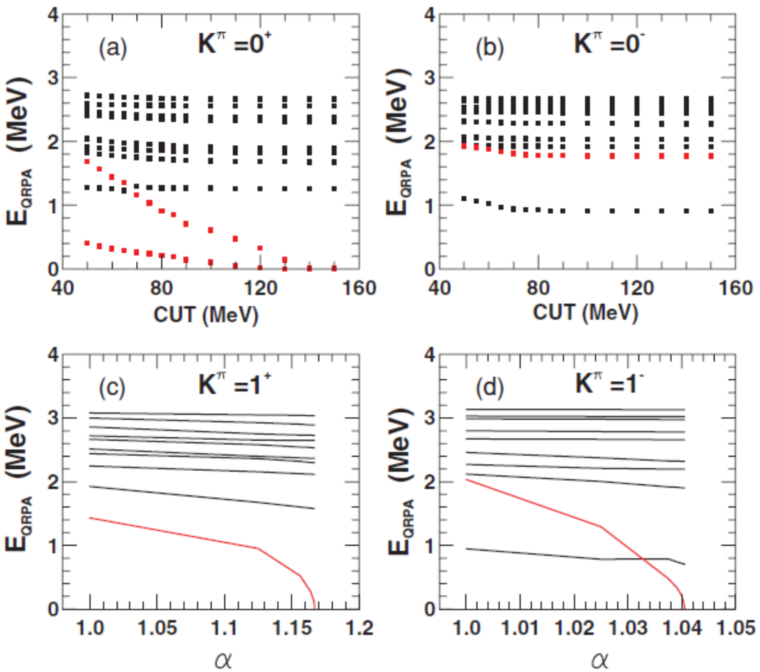

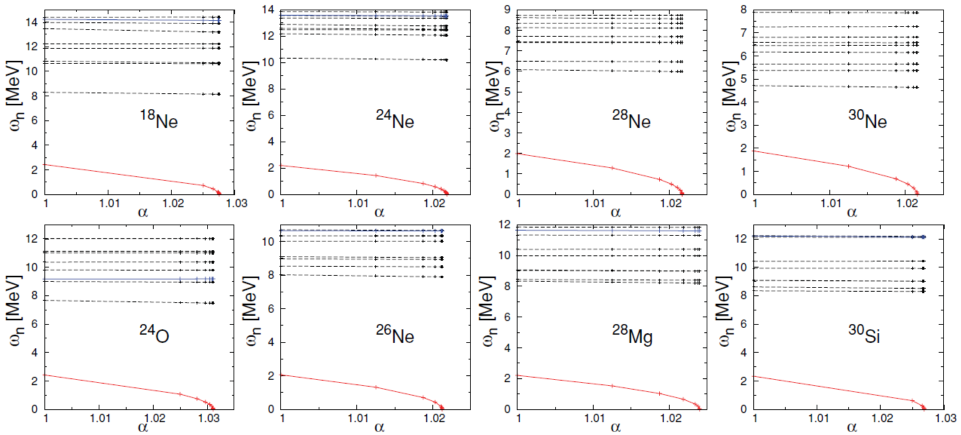

PHYSICAL REVIEW C **83**, 034309 (2011)

Low-energy dipole excitations in neon isotopes and $N = 16$ isotones within the quasiparticle random-phase approximation and the Gogny force

M. Martini, S. Péru, and M. Dupuis

Impact of cutoff on spurious mode

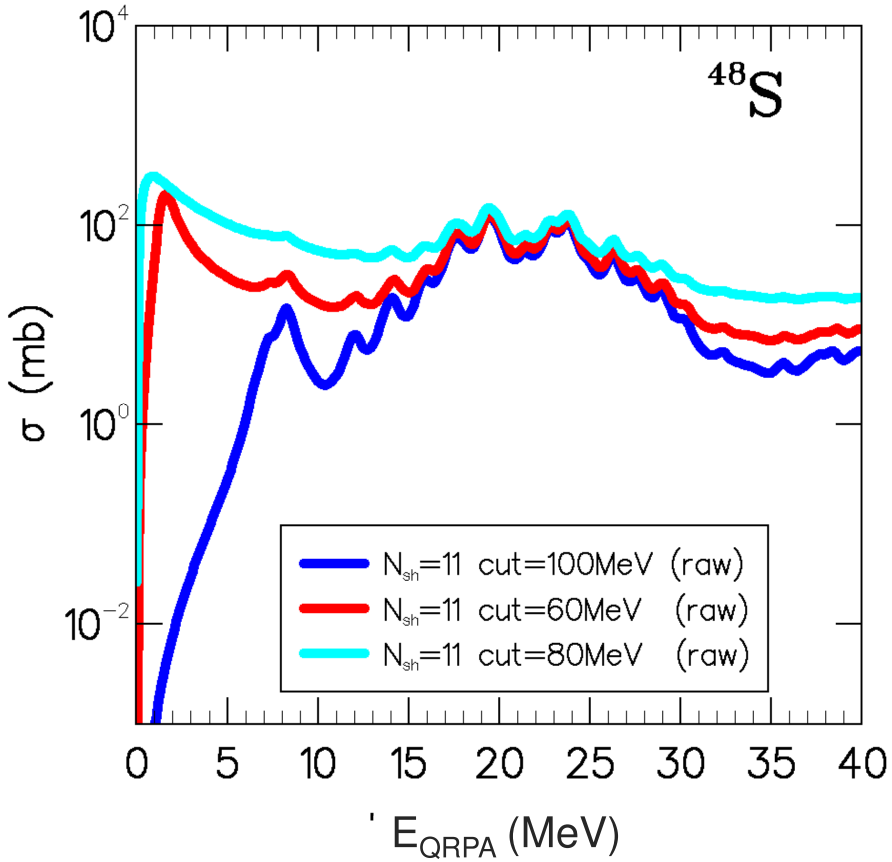

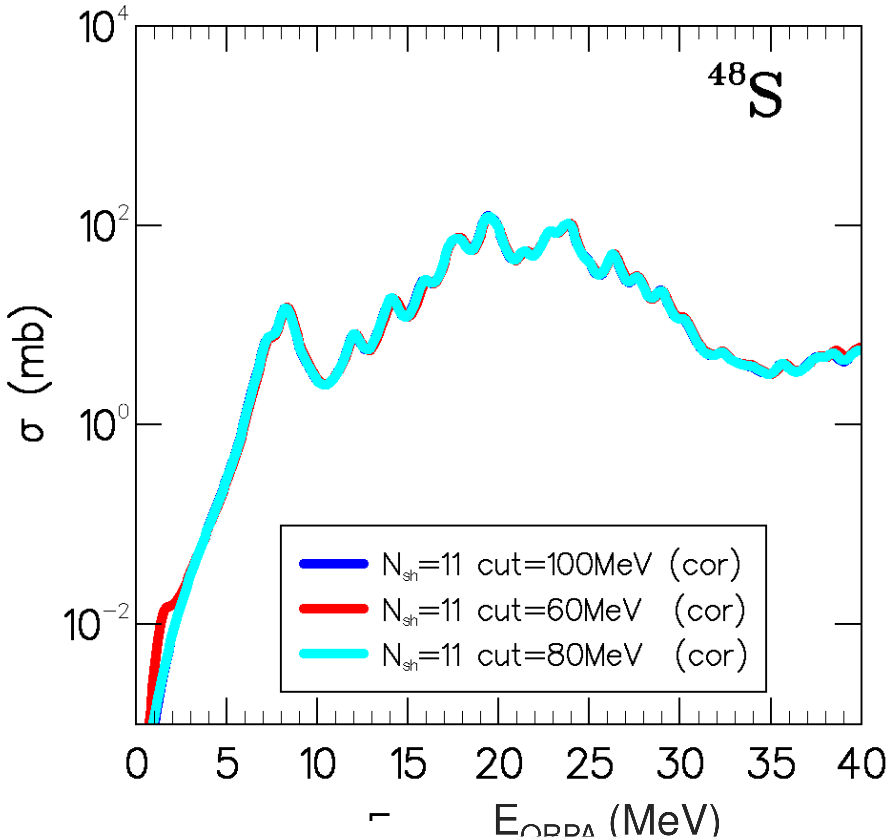

$$\hat{Q}_{E1} = e\sum_{p=1}^{Z} r_p Y_{1M}(\hat{r}_p).$$

$$D = \frac{Z}{A}\sum_{n=1}^{N} r_n Y_{1M}(\hat{r}_n) - \frac{N}{A}\sum_{p=1}^{Z} r_p Y_{1M}(\hat{r}_p),$$

Alternative resolution of QRPA equations

Full matrix filling and diagonalization

Both excitations energies and phonon wave functions are obtained as eigenvalues and eigenvectors.

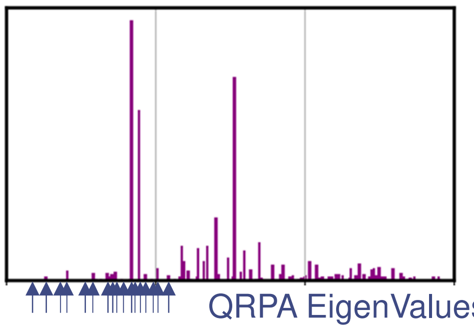

Require optimized codes running on supercomputers to reduce the “human” computational time and to share the available cpu memory.

Finite amplitude method (FAM) :

Self-consistent Iterative process to provide multipolar smoothed response function

Each point of the curve is the solution of one QFAM run

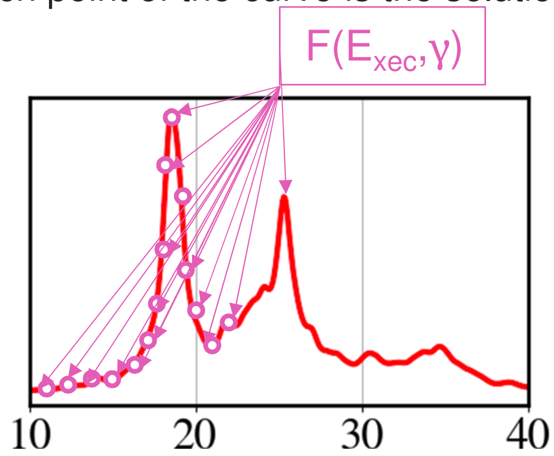

Smearing dependent ! $\omega \to \omega + i\gamma/2$

FAST production of multipolar response, but only the response. Eigen mode wave functions require additional treatment.

Talks of M. Frosini and Luis Gonzalez-Miret Zaragoza

2. QRPA for deformed nuclei

QRPA in axial symetry

$$\begin{pmatrix} A & B \\ B & A \end{pmatrix} \begin{pmatrix} X_n \\ Y_n \end{pmatrix} = \omega_n \begin{pmatrix} X_n \\ -Y_n \end{pmatrix}$$

$$\theta^+_{n,K} = \sum_{i<j} X^{ij}_{n,K} \eta^+_{i,k_i} \eta^+_{j,k_j} - (-)^K Y^{ij}_{n,K} \eta_{j,-k_j} \eta_{i,-k_i}$$

$$|JM(K)_n\rangle = \frac{\sqrt{2J+1}}{4\pi} \int d\Omega\, \mathcal{D}^J_{MK}(\Omega) R(\Omega) |\theta_n, K\rangle + (-)^{J-K} \mathcal{D}^J_{M-K}(\Omega) R(\Omega) |\theta_{\overline{n}}, -K\rangle$$

$$|\tilde{O}_{(J^\pi=0+)}\rangle = \frac{1}{2\pi} \int d\Omega \mathcal{D}^0_{00}(\Omega) R(\Omega) |0_{def}\rangle$$

$$\hat{Q}_{\lambda\mu} = r^\lambda Y_{\lambda\mu}$$

$$Y_{\lambda\mu} = \sum_{\mu'} \mathcal{D}^{*\lambda}_{\mu\mu'} Y_{\lambda\mu'}$$

$$\langle \tilde{O}_{(J^\pi=0+)} | \hat{Q}_{10} | JM(K=|1|)\rangle = -\frac{1}{\sqrt{3}} \left(\langle 0_{def} | \hat{Q}_{11} | \theta_n, K=1\rangle + \langle 0_{def} | \hat{Q}_{1-1} | \theta_n, K=-1\rangle \right)$$

$$\langle \tilde{O}_{(J^\pi=0+)} | \hat{Q}_{10} | JM(K=0)\rangle = \frac{1}{\sqrt{3}} \langle 0_{def} | \hat{Q}_{10} | \theta_n, K=0\rangle$$

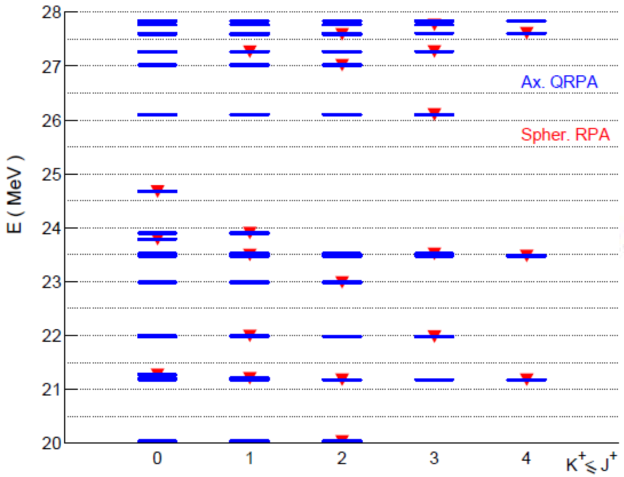

$$\rho^{Tr.}_{n,K}(\mathbf{r},\sigma) = \sum_{\alpha\beta} \Psi^*_\alpha(\mathbf{r},\sigma) \Psi_\beta(\mathbf{r},\sigma) \langle \tilde{0} | c^+_\alpha c_\beta | \theta_{n,K}\rangle$$

$$= \sum_{\alpha\beta} \Psi^*_\alpha(\mathbf{r},\sigma) \Psi_\beta(\mathbf{r},\sigma) \sum_{ij} \Big[X^{ij}_{n,K} (U^*_{\beta i} V_{\alpha j} - V_{\alpha i} U^*_{\beta j}) + (-)^{K+1} Y^{ij}_{n,K} (U_{\alpha i} V^*_{\beta j} - V^*_{\beta i} U_{\alpha j}) \Big]$$

whatever the intrinsic deformation of the ground state

Potential Energy Surfaces

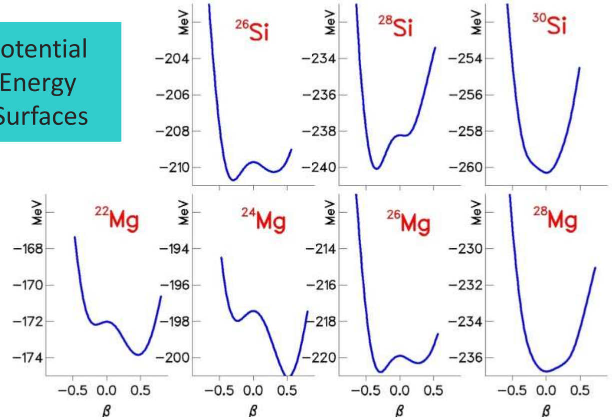

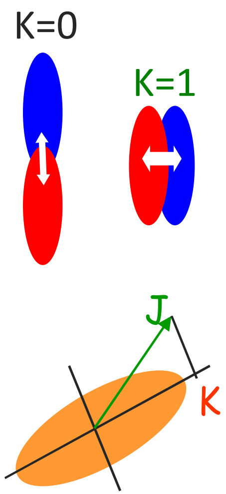

IV Dipole

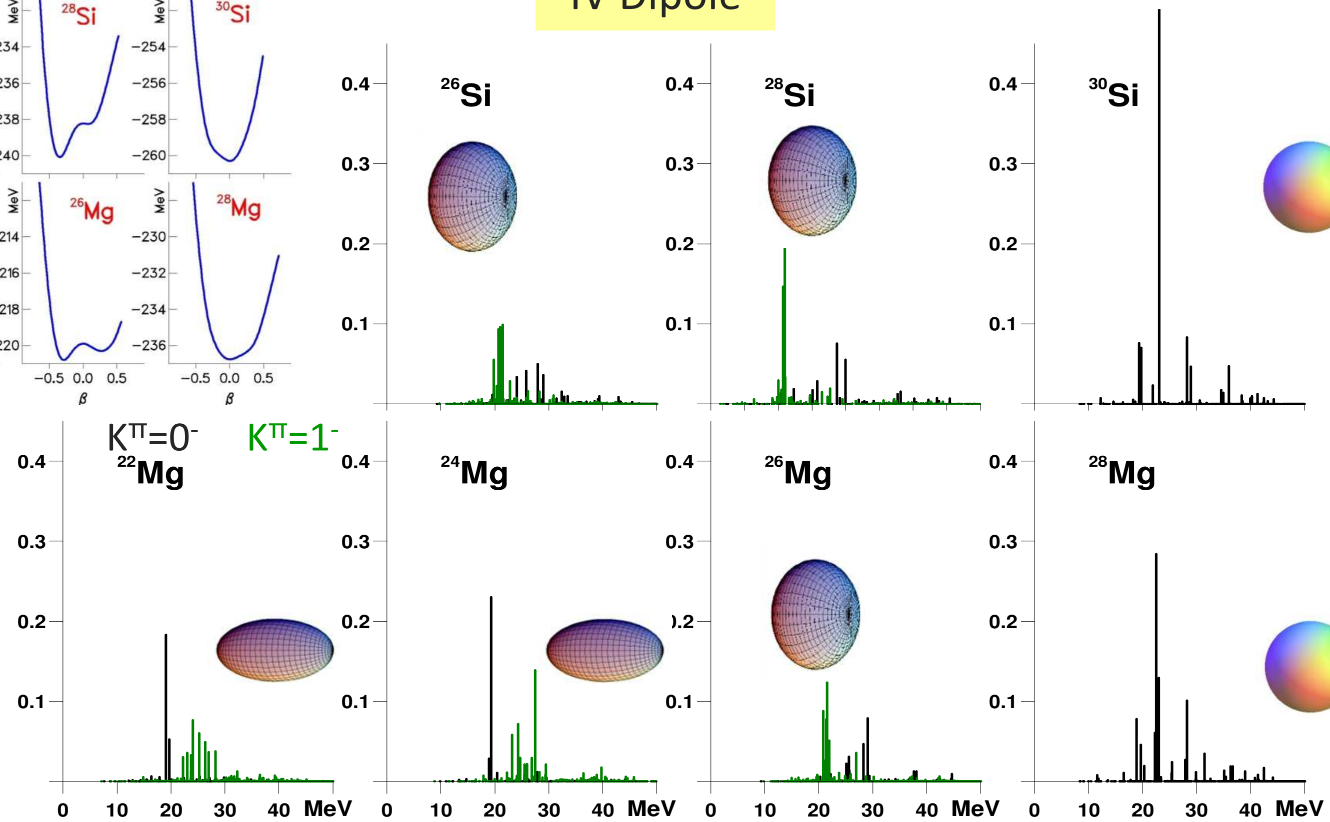

“First study” with QRPA in axial symmetry

S. Péru and H. Goutte, Phys. Rev. C 77, 044313 (2008).

Investigation of the isoscalar response of ^{24}Mg to ^{6}Li scattering

FIG. 2. ISGMR strength function.

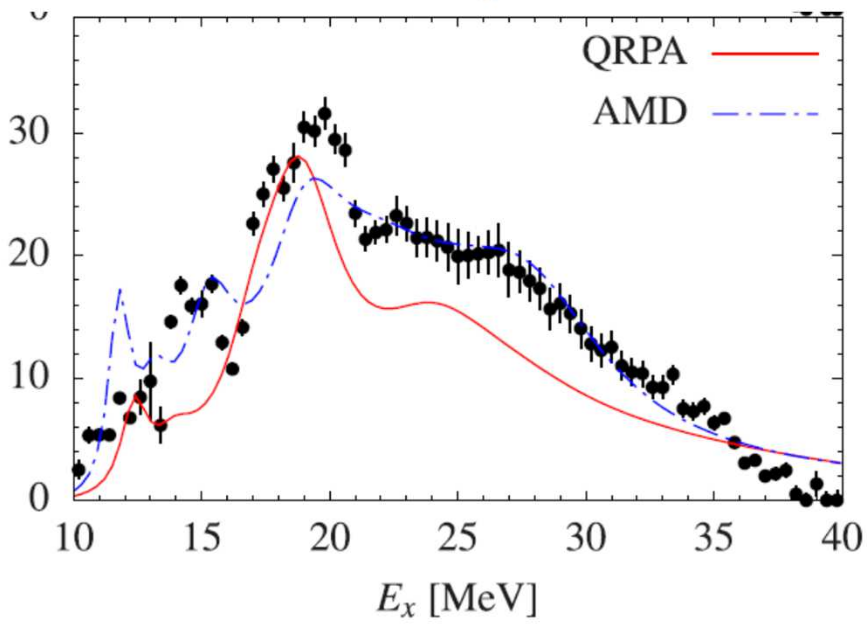

QRPA distribution was shifted upward by 2 MeV.

FIG. 4. ISGQR strength function.

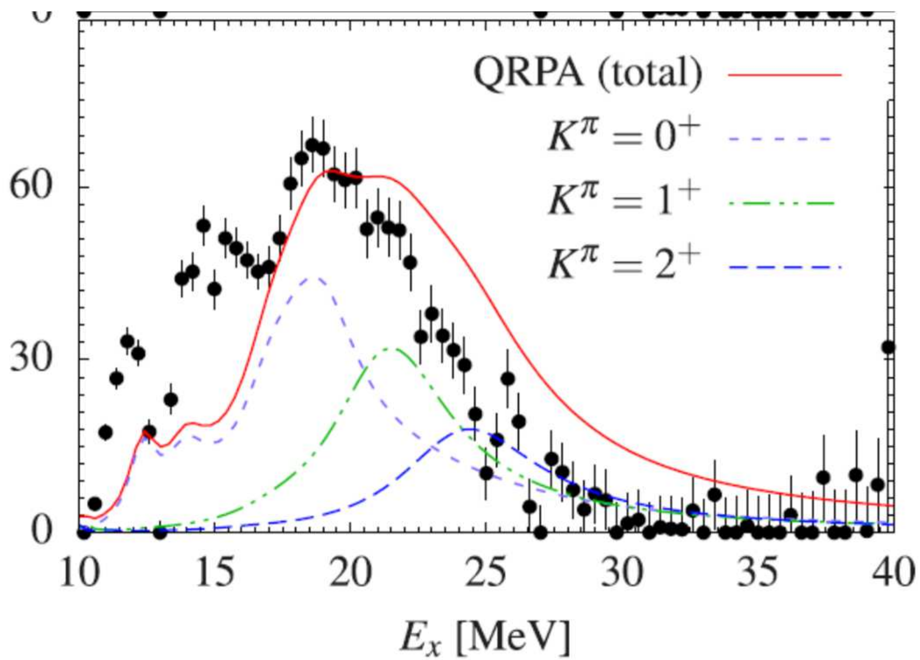

Comparison with QRPA calculations showing the respective $K^\pi = 0^+$, 1^+, and 2^+ components. The QRPA distributions were shifted upward by 2 MeV.

J. C. Zamora et al, PRC 104, 014607 (2021)

Intrinsic transition density and radial transition by multipolar expansion

$$\rho^{n,K}(\vec{r}) = \sum_{\alpha\beta} \phi^*_\alpha(\vec{r})\phi_\beta(\vec{r})\, \langle\hat{\theta}_n, K|c^\dagger_\alpha c_\beta|\tilde{0}\rangle,$$

$$\rho^{n,K}_J(r) = \int d\Omega\, \rho^{n,K}(\vec{r})\, Y_{JK}(\Omega),$$

$$Z^{n,K}_{\alpha,\beta} \equiv \langle\hat{\theta}_n, K|c^\dagger_\alpha c_\beta|\tilde{0}\rangle.$$

$$Z^{n,K}_{\alpha,\beta} = \sum_{i<j}\Big[X^{ij}_{n,K}\,(U_{\alpha i}V_{\beta j} - U_{\alpha j}V_{\beta i}) + Y^{ij}_{n,K}\,(V_{\alpha j}U_{\beta i} - V_{\alpha i}U_{\beta j})\Big].$$

$$\langle\hat{\theta}_n, K|\hat{Q}_{\lambda\mu}|\tilde{0}\rangle = \sum_{\alpha\beta}\langle\alpha|\hat{Q}_{\lambda\mu}|\beta\rangle\, Z^{n,K}_{\alpha,\beta},$$

E. V. Chimanski et al, submitted…

$$\widehat{Q}_{\lambda\mu} = \int \rho(\vec{r})r^\lambda Y_{\lambda\mu}(\theta,\varphi)d^3r$$

$$\delta\rho(R,\theta,\varphi) = \langle 0|\widehat{\rho}|n\rangle\,,\ \forall n.$$

$$B(E_{\lambda\mu}, J_i \to J_f) = \frac{1}{2J_i+1}|\,\langle J_f|\,\widehat{Q}_{\lambda\mu}\,|J_i\rangle\,|^2.$$

$$\delta\rho(R,\theta,\varphi) = \sum_{L=0}^{\infty}\sum_{M=-L}^{L}\delta\rho_{LM}(R)\times Y_{LM}(\theta,\varphi).$$

$$B(E_{\lambda K}) = \left|\int dr \times \delta\rho_{\lambda K}(R)\times r^a\right|^2 \quad \text{with} \quad \begin{cases} a = 4 \text{ if } \lambda = 0 \\ a = \lambda + 2 \text{ if } \lambda \neq 0 \end{cases}.$$

F. Clayes, 2018

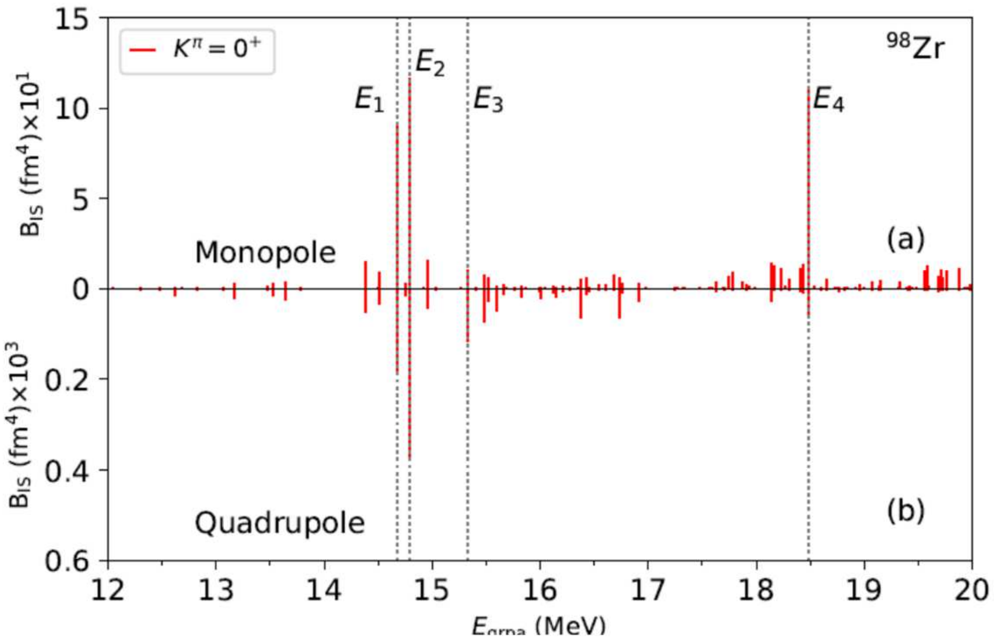

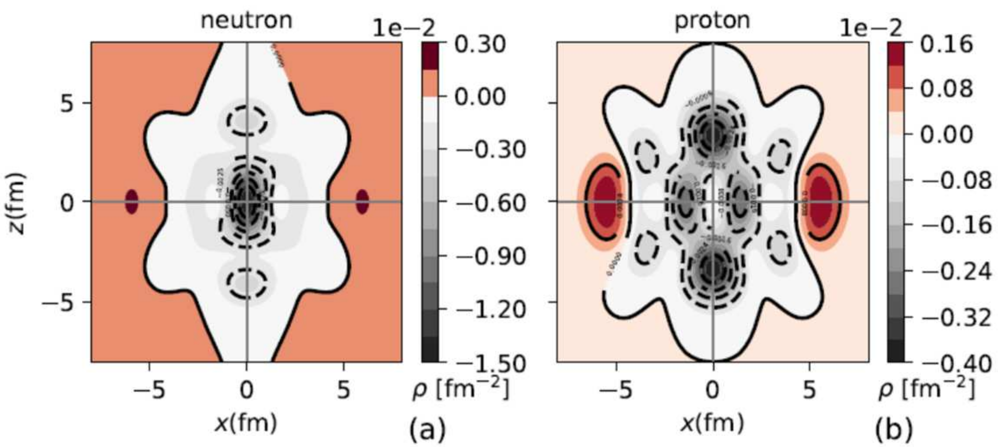

Intrinsic transition density for E1=14,68 MeV.

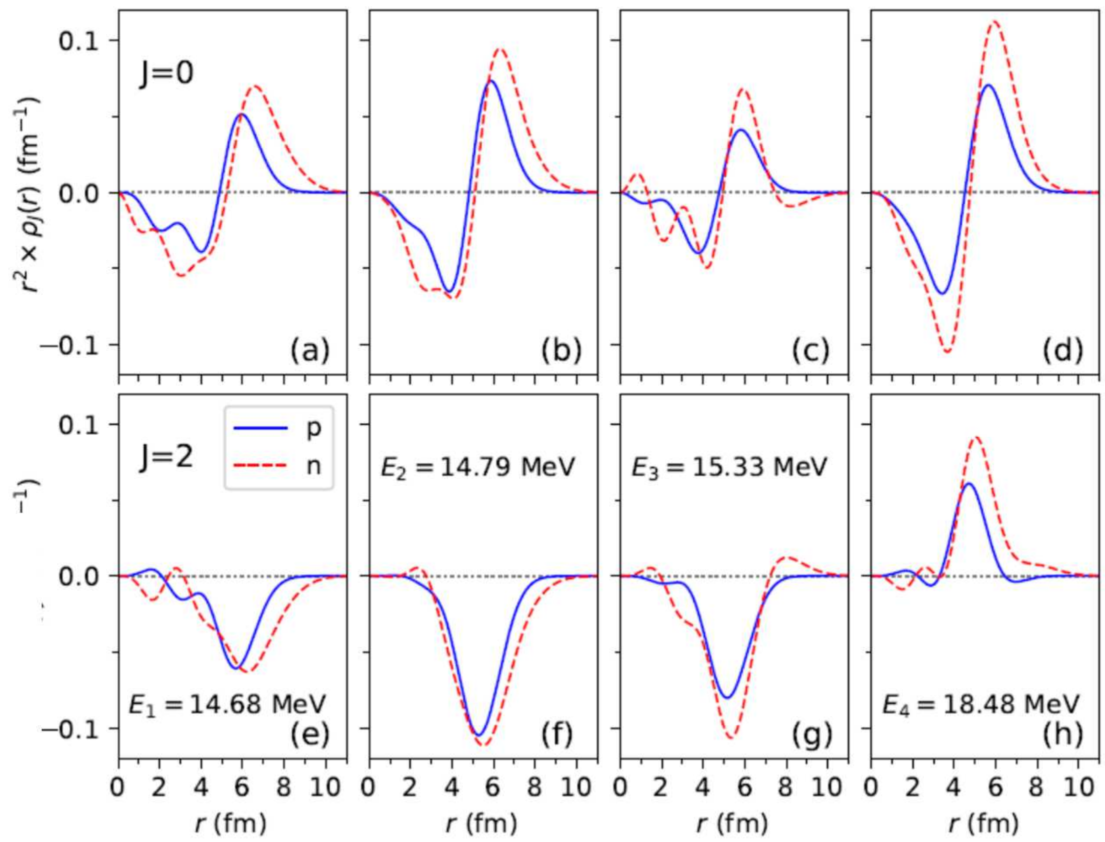

E. V. Chimanski et al,
arXiv:2308.13374v2 **[nucl-th]**

Pure monopole K=0, J=0

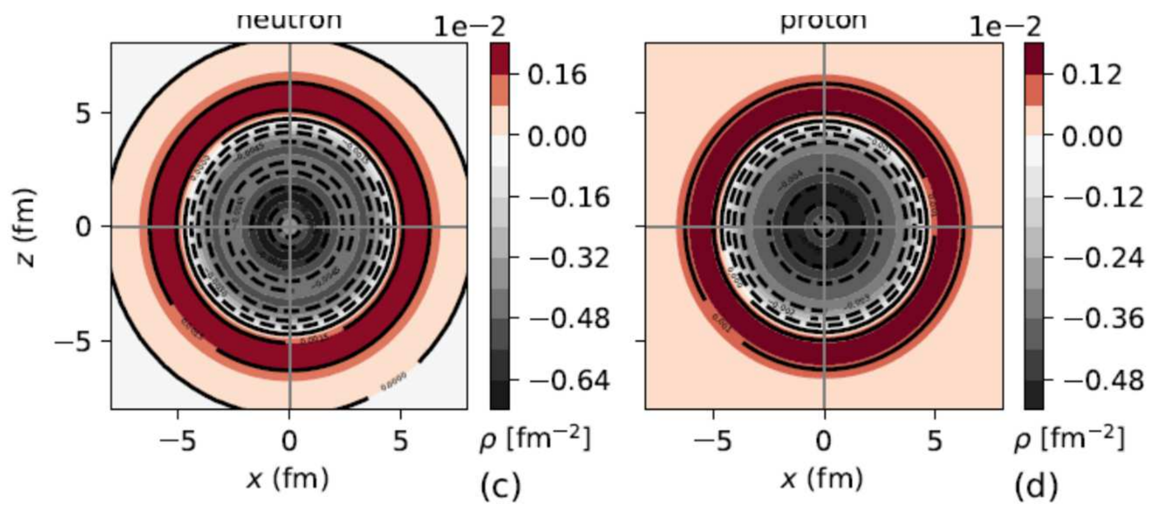

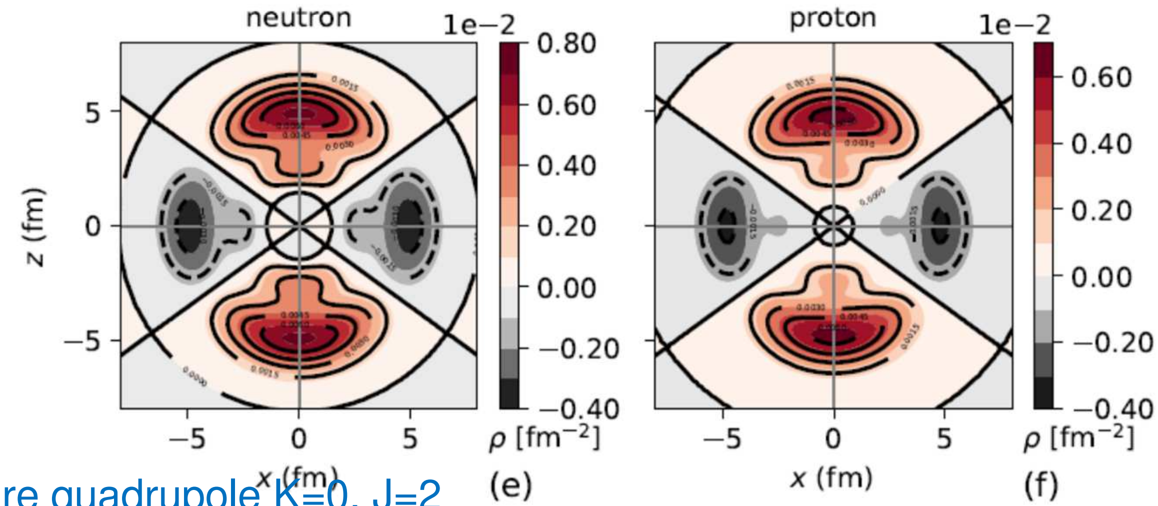

Pure quadrupole K=0, J=2

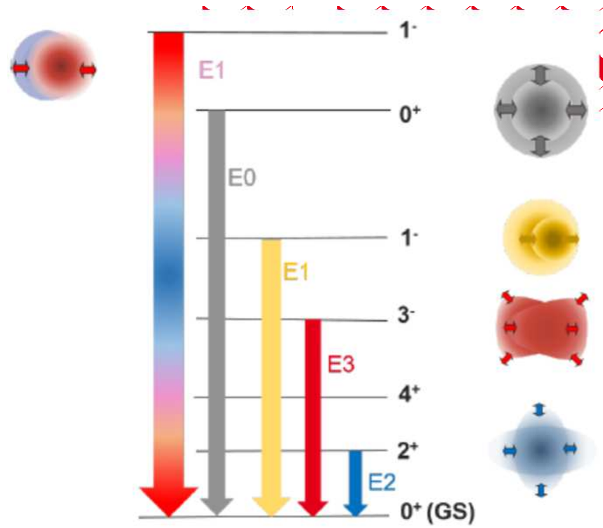

E. V. Chimanski et al, arXiv:2308.13374v2 **[nucl-th]**

Pure Dipole

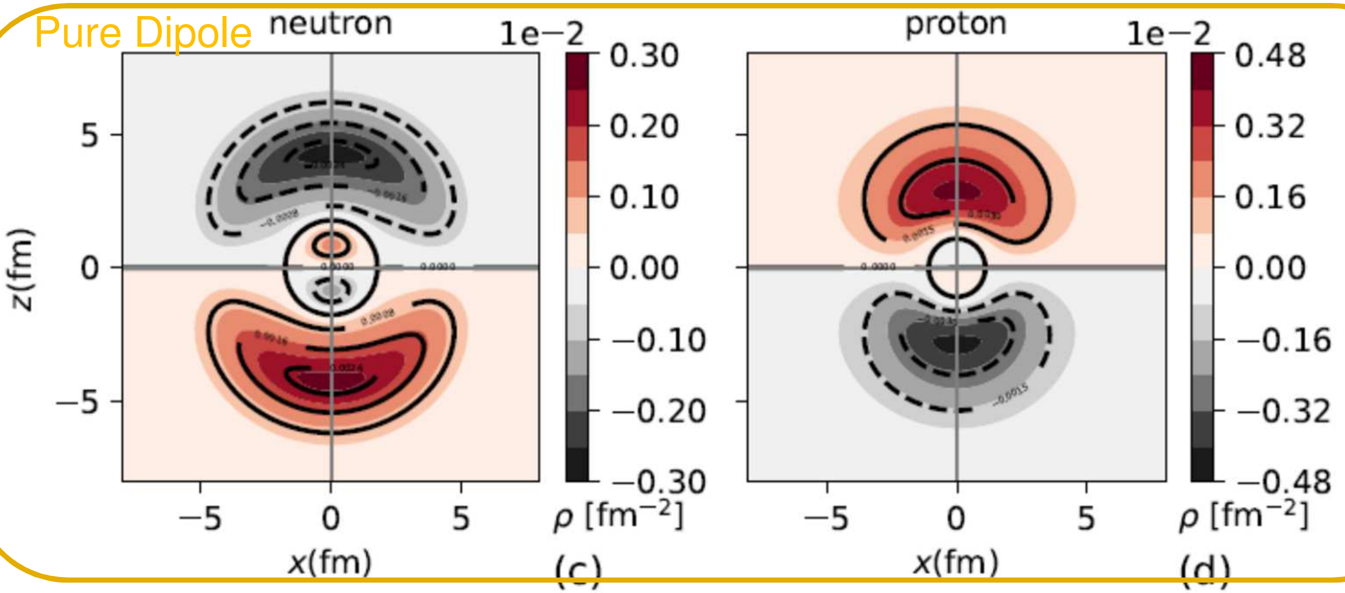

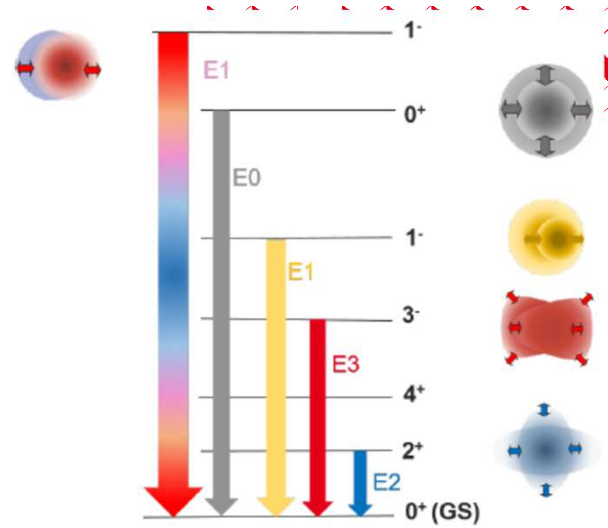

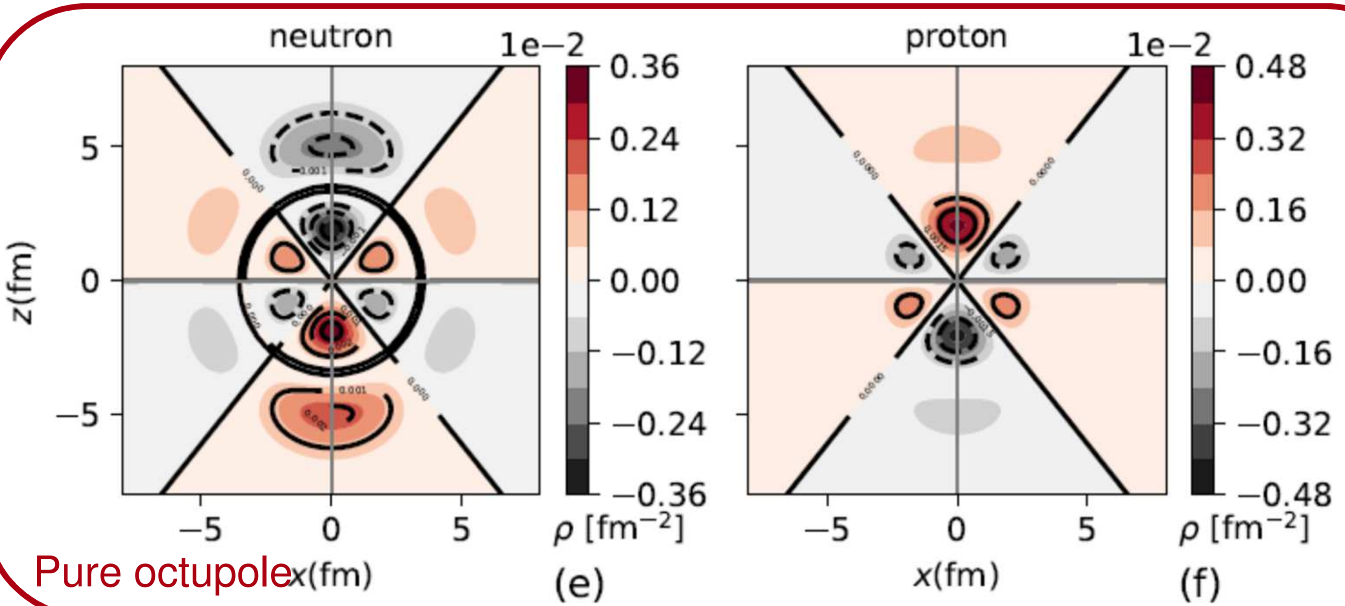

Pure octupole

E. V. Chimanski et al, arXiv:2308.13374v2 **[nucl-th]**

3. Some systematic QRPA calculations

D1M HFB+QRPA in axial symmetry applied to E1 and M1 strength

Magnetic and electric modes on the same footing

Impact of the deformation

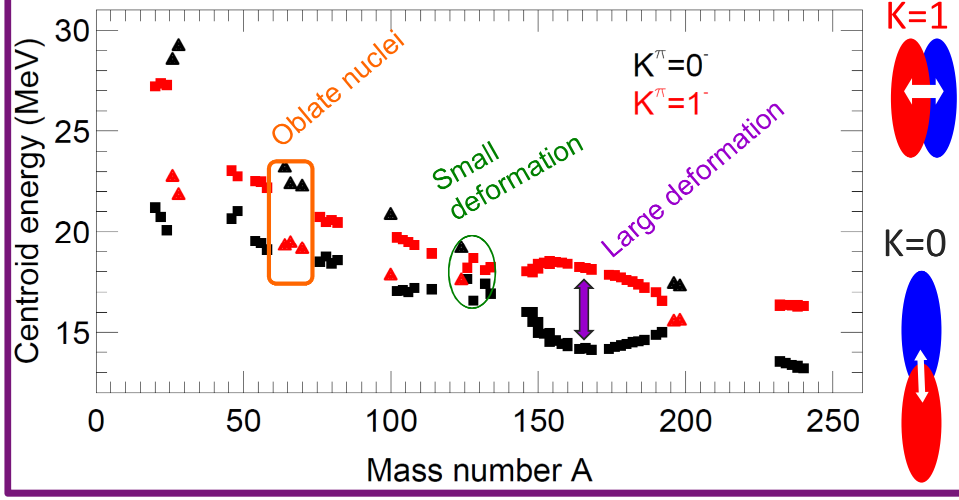

[M. Martini et al, PRC 94, 014304 (2016)]

Spherical nuclei
One Lorentzian in RIPL

Deformed nuclei
Two Lorentzians in RIPL

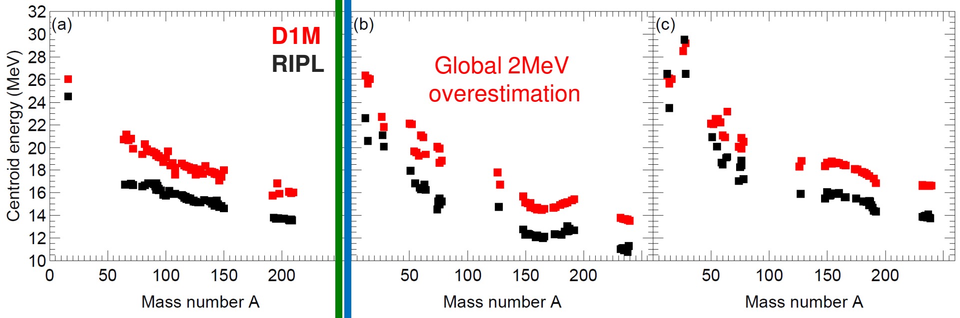

S. Goriely et al, PRC 94, 044306 (2016

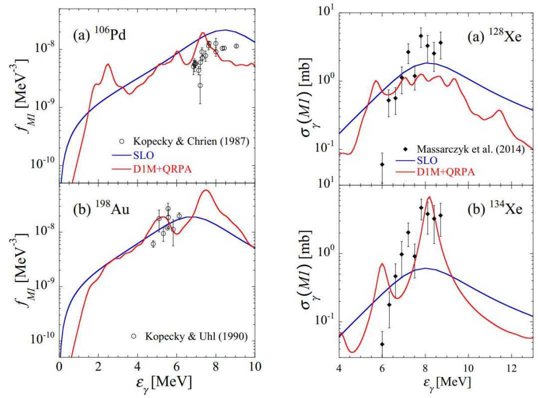

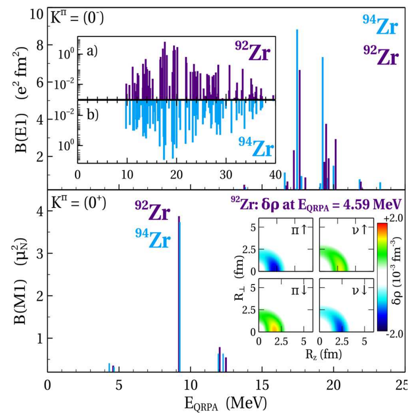

Gogny-HFB + QRPA

[S. Goriely et al, PRC98,014327 (2018)]

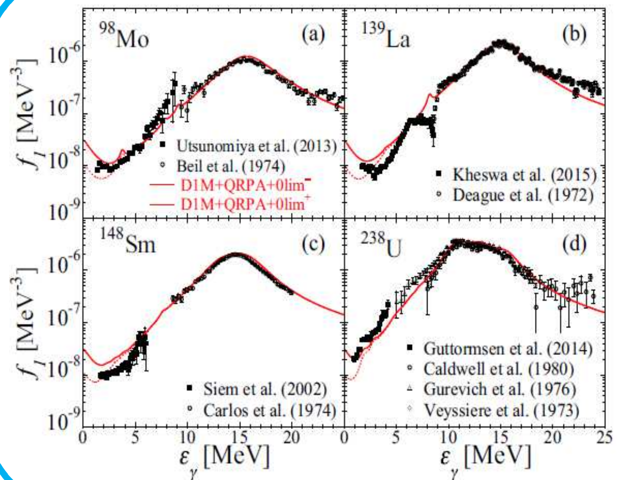

QRPA B(E1) and B(M1)

- Lorentzian folding
- shift in energy to fit data

Phenomenological **upbend** inspired by shell model for the decay strength

Global trend : D1S versus D1M

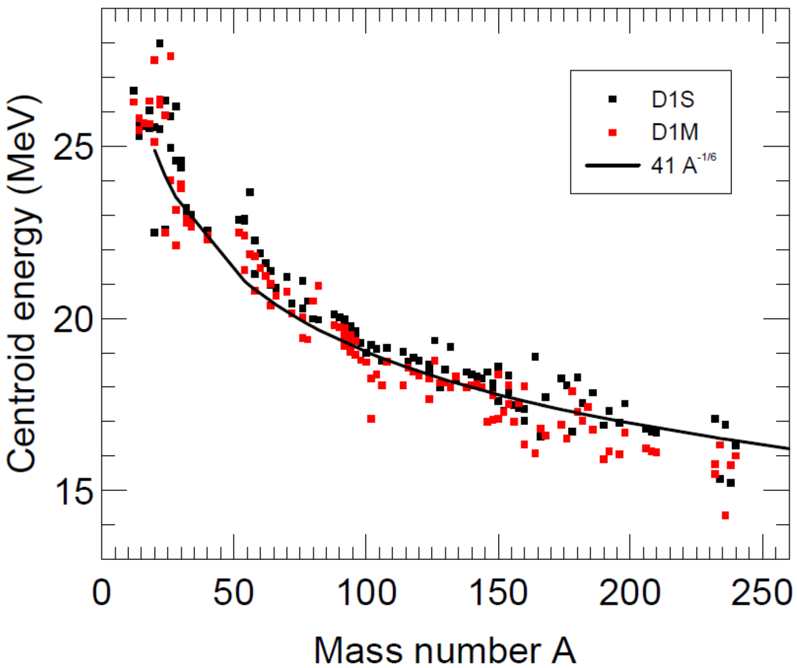

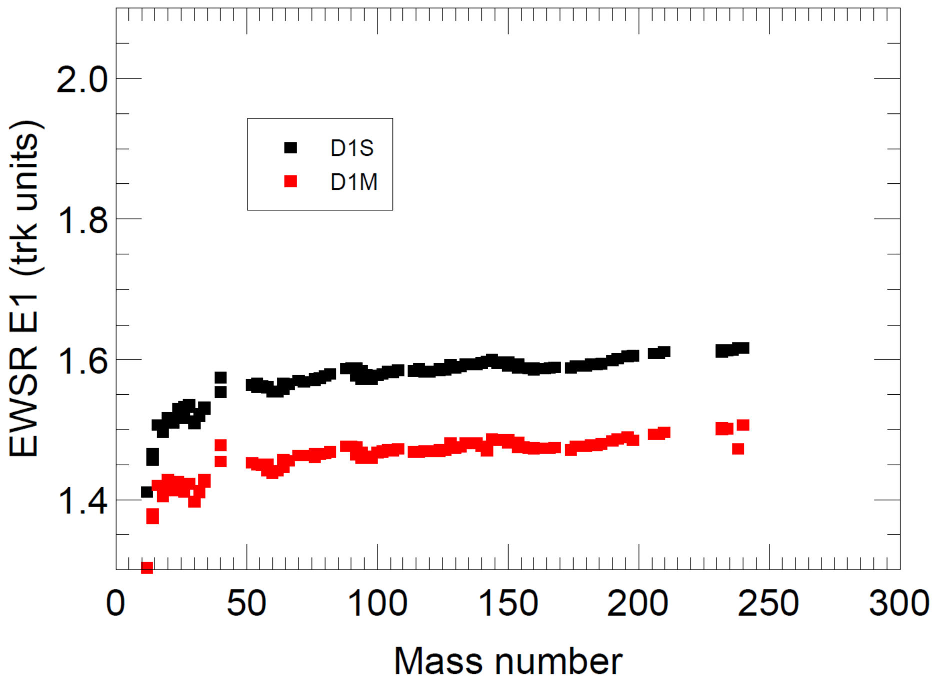

A few 100 keV overestimation of the D1S centroid energies with respect to D1M ones leads to a 0,2 shift of the EWSR (in TRK units).

M. Martini et al, PRC 94, 014304 (2016)

4. QRPA for odd nuclei

Even-Even or standard quasi boson

$$\theta_n^+ = \sum_{i<j} X_n^{ij} \eta_i^+ \eta_j^+ - Y_n^{ij} \eta_j \eta_i$$

$$\eta_i^+ |GS_{HFB}> = \eta_i^+ |0_{qp}> = |i>,$$
$$\eta_i |GS_{HFB}> = \eta_i |0_{qp}> = 0 \quad \forall i.$$

$$\beta_i |0_{qp}> = 0 \quad \forall i,$$
$$\beta_b^+ |0_{qp}> = |GS_b>,$$
$$\beta_b |GS_b> = |0_{qp}>,$$
$$\beta_i |GS_b> = 0 \ \forall i \neq b.$$

$$\eta_i = \beta_i \ \forall i \neq b,$$
$$\eta_i^+ = \beta_i^+ \ \forall i \neq b,$$
$$\eta_b = \beta_b^+,$$
$$\eta_b^+ = \beta_b$$

Generalized quasi boson

$$\theta_n^+ = \sum_{b \neq i < j \neq b} \{X_n^{ij} \beta_i^+ \beta_j^+ - Y_n^{ij} \beta_j \beta_i\}$$

Blocking QRPA

$$+ \sum_{i<j=b} \{X_n^{ib} \beta_i^+ \beta_b - Y_n^{ib} \beta_b^+ \beta_i\}$$
$$+ \sum_{i=b<j} \{X_n^{bj} \beta_b \beta_j^+ - Y_n^{bj} \beta_j \beta_b^+\}$$

“Unlock“ including swap configurations

On top of the HFB calculations with blocking, axially symmetric QRPA calculations are performed. A main difference with respect to even-even nuclei is the non-zero value of the ground state spin K_1. In the following, K_2 corresponds to the final state.

here that we exclude from the QRPA valence space the qp orbital which is blocked in the HFB ground state.

S. Goriely, S.P., G. Colo, et al, PRC102, 064309, 2020

1. Deformed odd nuclei

$$\langle J_2||O_\lambda||J_1\rangle = \sqrt{(2J_1+1)(2J_2+1)}\Bigg[(-)^{J_2-K_2}\begin{pmatrix} J_2 & \lambda & J_1 \\ -K_2 & \mu & K_1 \end{pmatrix}\langle \Phi_{K_2}|O_{\lambda\mu}|\Phi_{K_1}\rangle + (-)^{J_2-K_2}\begin{pmatrix} J_2 & \lambda & J_1 \\ -K_2 & \mu' & -K_1 \end{pmatrix}(-)^{J_1-K_1}\langle \Phi_{K_2}|O_{\lambda\mu'}|\Phi_{-K_1}\rangle\Bigg].$$

2. Spherical odd nuclei

$$\langle J_2||O_\lambda||J_1\rangle = \frac{(-)^{1-J_2-K_2}}{\sqrt{2J_1+1}}\begin{pmatrix} J_2 & \lambda & J_1 \\ K_2 & \mu & -K_1 \end{pmatrix}^{-1}\langle \Phi_2|O_{\lambda\mu}|\Phi_1\rangle.$$

S. Goriely, S.P., G. Colo, et al, PRC102, 064309, 2020

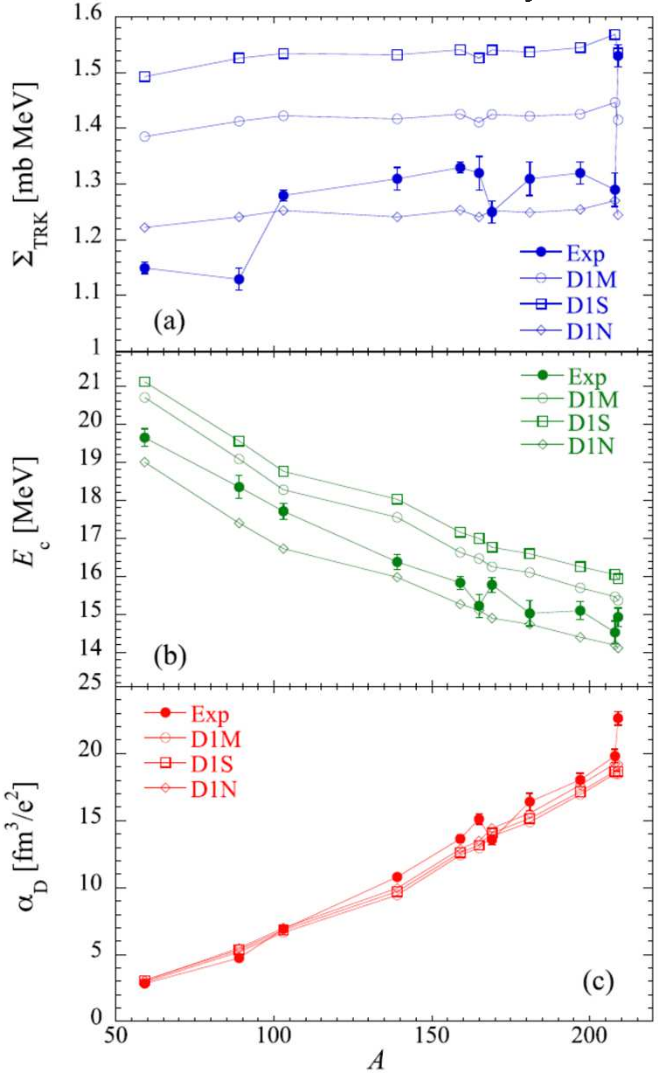

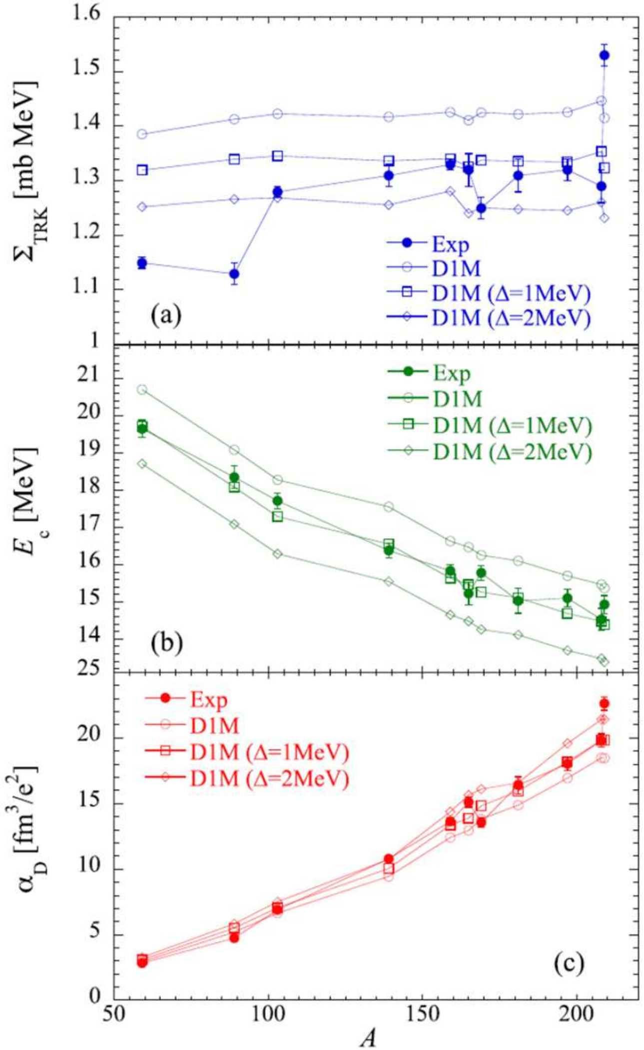

Systematics of the 5/2+ level in N=151 isotones

QRPA $J^{\pi} = 5/2^{+}$ state is defined as a phonon $K^{\pi}=-2^{-}$
on the $K^{\pi}=-9/2^{-}$ ground state (blocking $\nu 9/2^{-}$ in HFB and in QRPA)

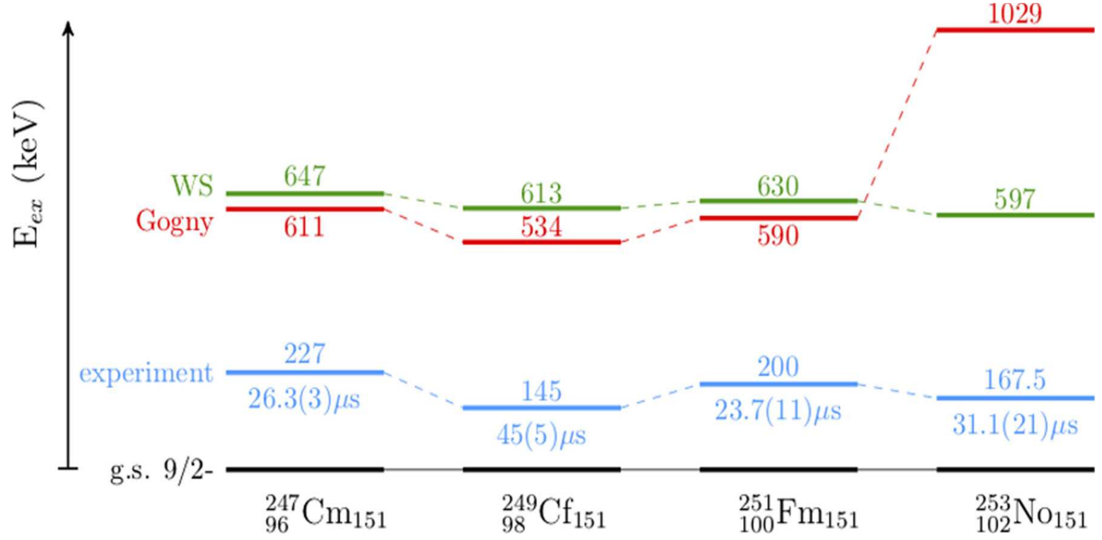

Nucleus	$E_{Exp.}$ keV	E_{D1M} keV	B(E3) Exp. W.u.	B(E3) D1M W.u.	% π	% ν
^{247}Cm	227	611	7.3(21)	9,8	15	85
^{249}Cf	145	534	10(4)	11,1	18	82
^{251}Fm	200	590	18(6)	9,2	13	87
^{253}No	168	(1029)	13(8)			

K. Rezynkina et al,Physical Review C 97,054332 (2018)

An alternative viewpoint on the nuclear structure towards ^{100}Sn: Lifetime measurements in ^{105}Sn

G. Pasqualato el al, PLB 845 (2023) 138148

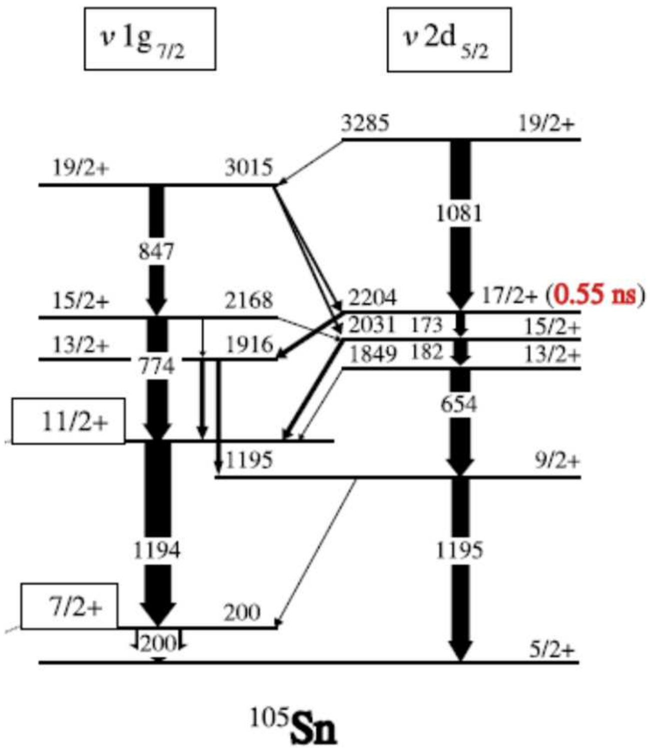

	exp	LSSM[(1)]	QRPA	MPMH
B(M1; $7/2^+ \rightarrow 5/2^+$) $[\mu_N^2]$	0.0107(6)	0.0017		0.0037
B(E2; $11/2^+ \rightarrow 7/2^+$) $[e^2 fm^4]$	50(15)	118	40	

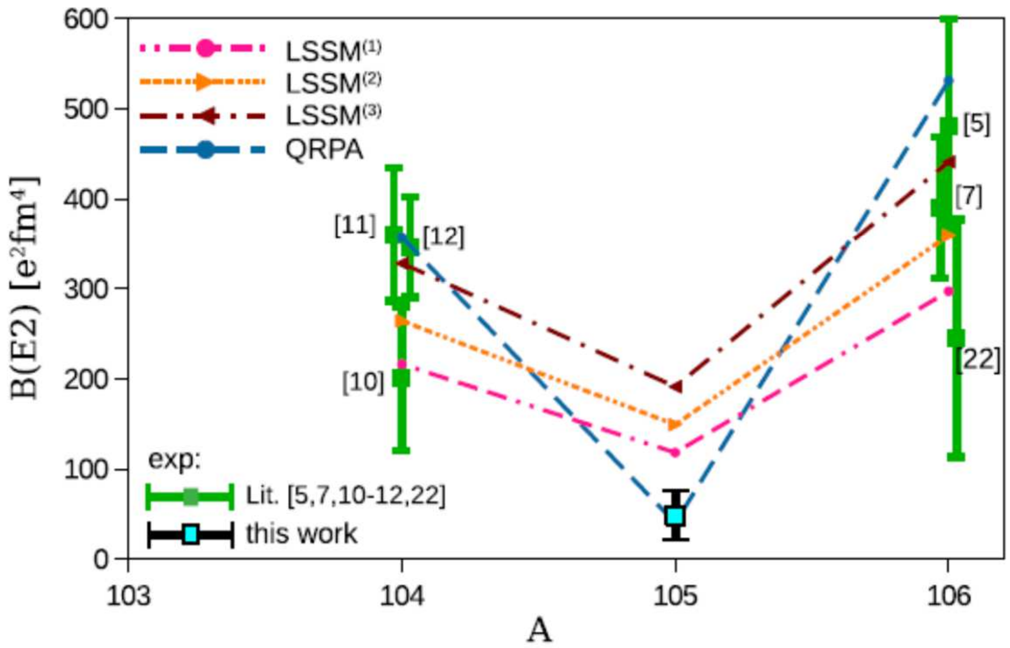

5 QRPA and its unusual application

Description of J= 4^{-} isomers in N=100 isotones

Unusual application: 4^- isomers in N=100 isotones

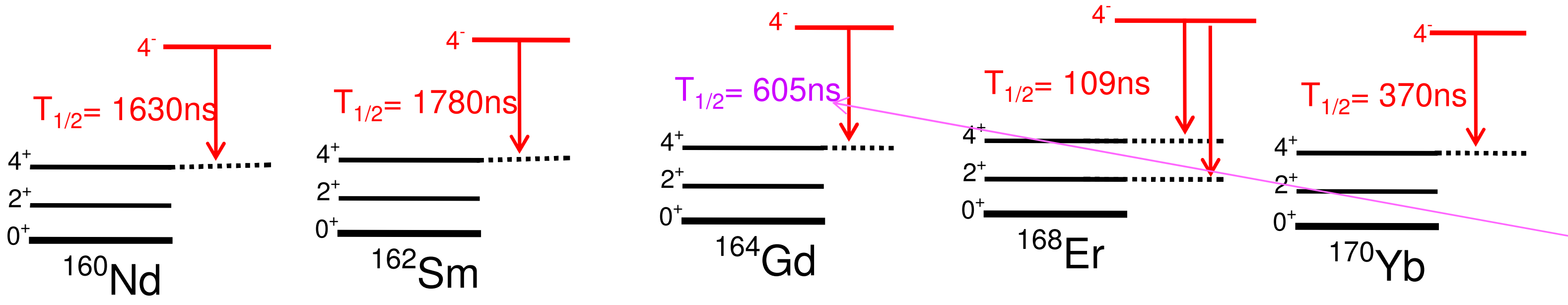

Experimental half-lives

Laurent Gaudefroy, CEA,DAM,DIF

Spontaneous fission of ^{252}Cf

The $4^- \rightarrow 4^+$ transition is expected to be E1

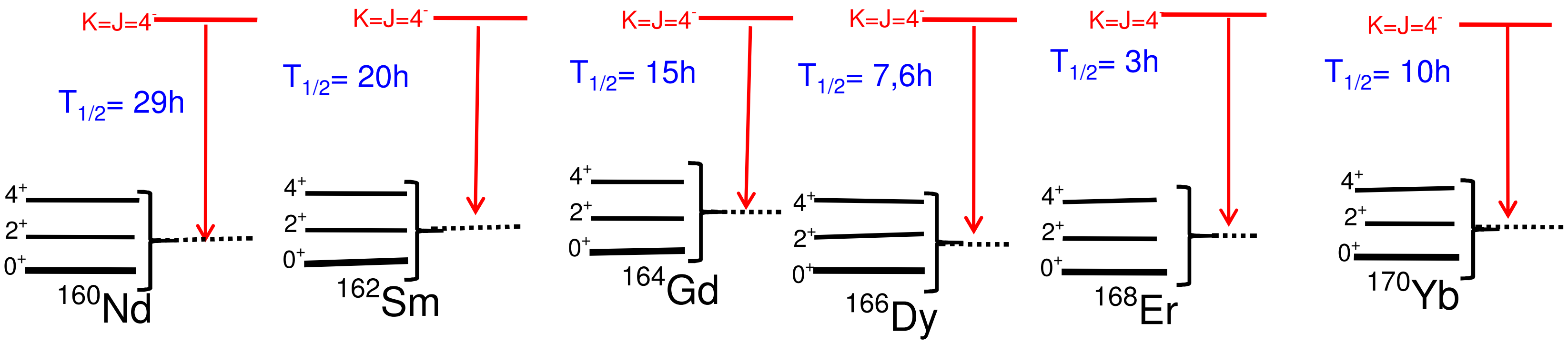

HFB+QRPA in axial symmetry with D1M Gogny force for $K^\pi = 4^-$

Only M4 and E5 transitions are allowed ← $\lambda \geq K=4$

L. Gaudefroy, S. Péru, et al, PRC97, 064317 (2018)

What is the nature of these J=4 isomers?

Example : ^{162}Sm

$T_{1/2}$= 1780ns

J=4, $K^{\pi}=0^{-}$	J=4, K=1	J=4, K=2	J=4, K=3	J=4, K=4
B(E1) B(M2)	B(E1) B(M2)	B(E3) B(M2)	B(E3) B(M4)	B(E5) B(M4)
$T_{1/2} \approx$ 0,5 ps	$T_{1/2} \approx$ 300 ps	$T_{1/2} \approx$ 20 ns	$T_{1/2} \approx$ 700 µs	$T_{1/2} \approx$ 20 h

No calculated half-live reproduces the experimental one.
A very small K=1 component in the wave function would explain the observations.

There are 3 main mechanisms for K admixture :
F. G. Kondev, G.D. Dracoulis and T. Kibedi, ADNDT 103, 50 (2015)

- High level density
- Triaxial shape
- Mixing with Coriolis interaction

to fix it:

$$< K \,|\, Hc \,|\, K{+}1 >= -\frac{\hbar}{2I}\sqrt{(J-K)(J+K+1)}\,< K |\, j^- | K{+}1 >$$

Then, we calculated relevant inter-band transitions:

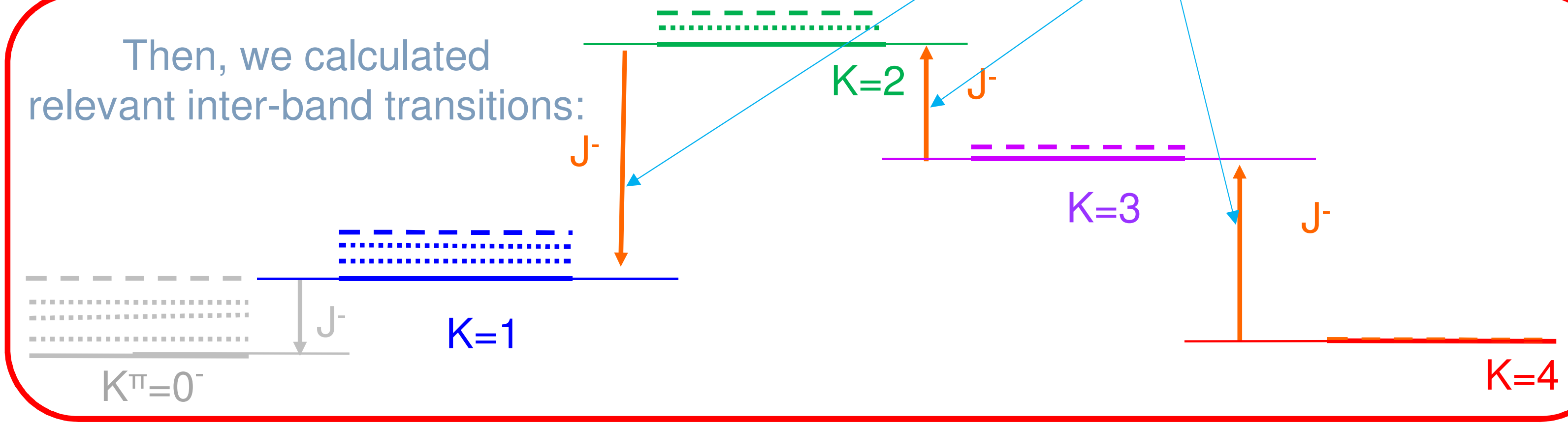

T ½ ns	^{160}Nd	^{162}Sm	^{164}Gd	^{166}Dy	^{168}Er	^{170}Yb	^{172}Hf
Exp.	1670(210)	1780(70)	605(30)	?	109(7)	370(15)	~1
QRPA	6970	11105	3980	285	365	260	1,5
QRPA/Exp.	4,17	6,24	6,57	?	3,35	0,703	1,5

L. Gaudefroy, S. Péru, et al, PRC97, 064317 (2018)

→ More transition probabilities are now available

Low energy spectroscopy
in spherical nuclei : $2^+_2 \rightarrow 2^+_1$
and $4^+_1 \rightarrow 2^+_1$ transition probabilities

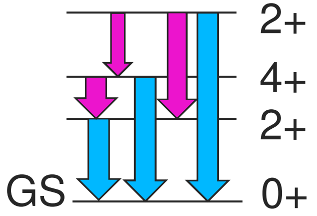

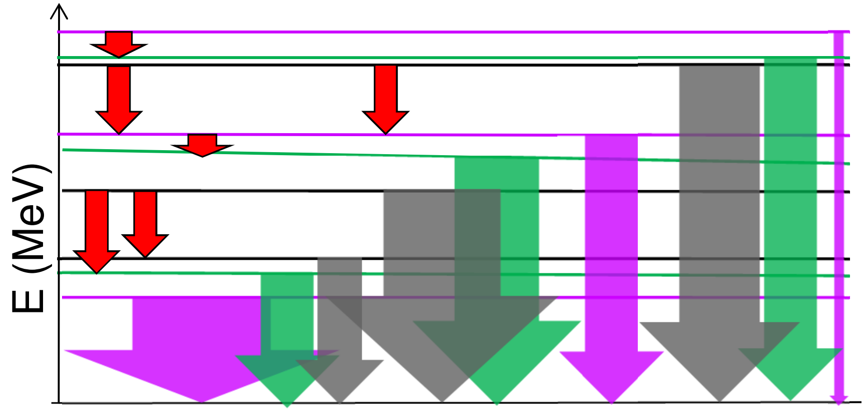

Theoretical description of « up-bend » :
increase of γ-ray strength function at low energy

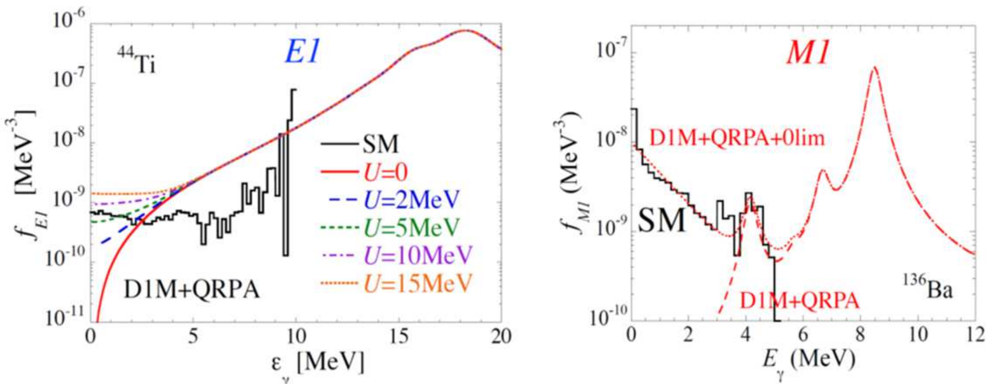

S. Goriely et al, PRC98,014327 (2018)

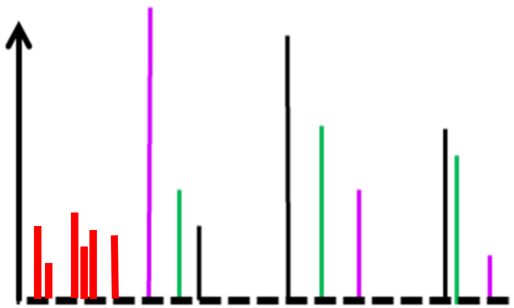

$E_\gamma \neq E_{exc}$

6. Some perspectives for γ-ray strength functions

Going back to the photon strength function definition !

Absorption versus decay

1/2

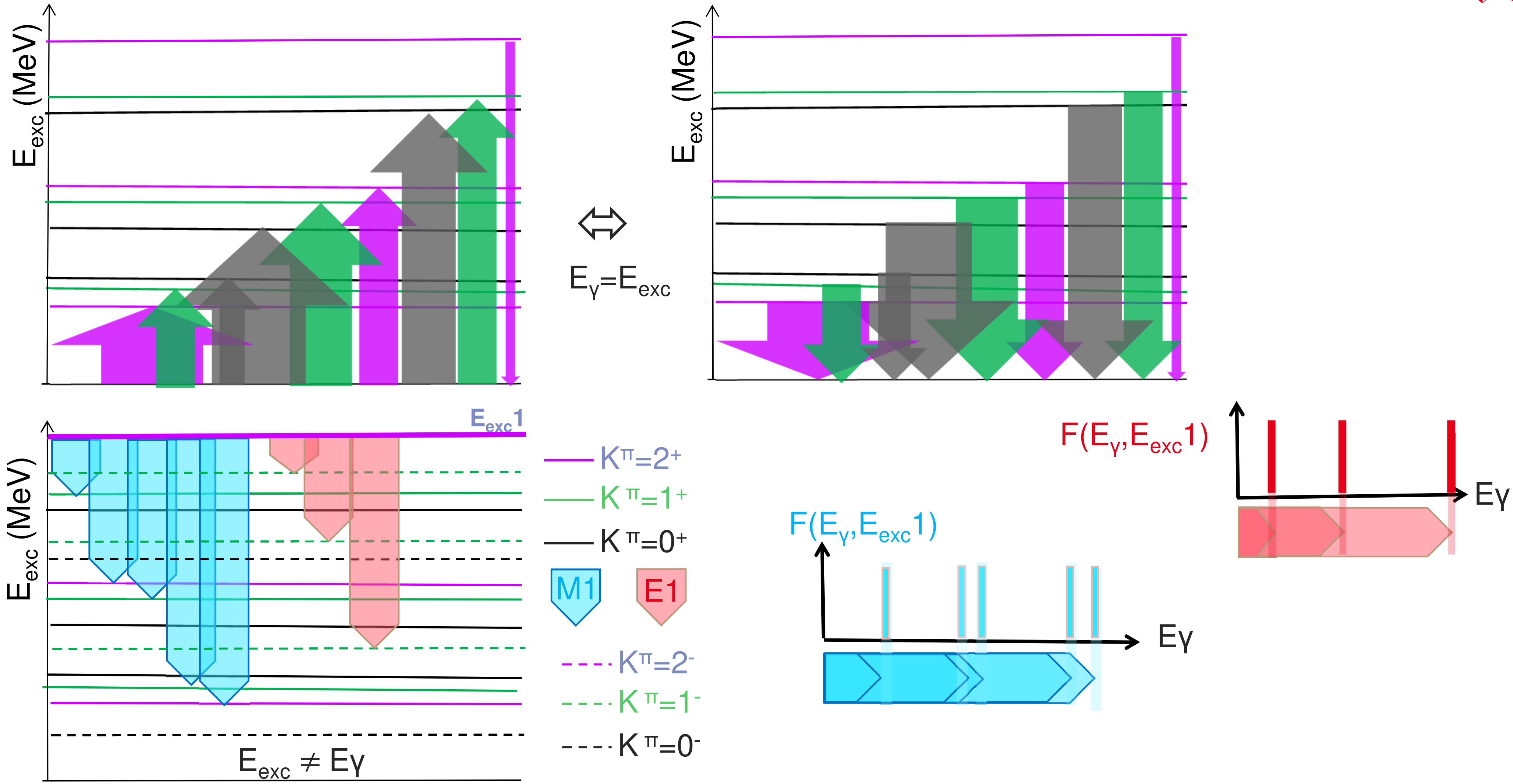

Absorption versus decay

The γ-ray strength function depends on the excitation energy and on the level density

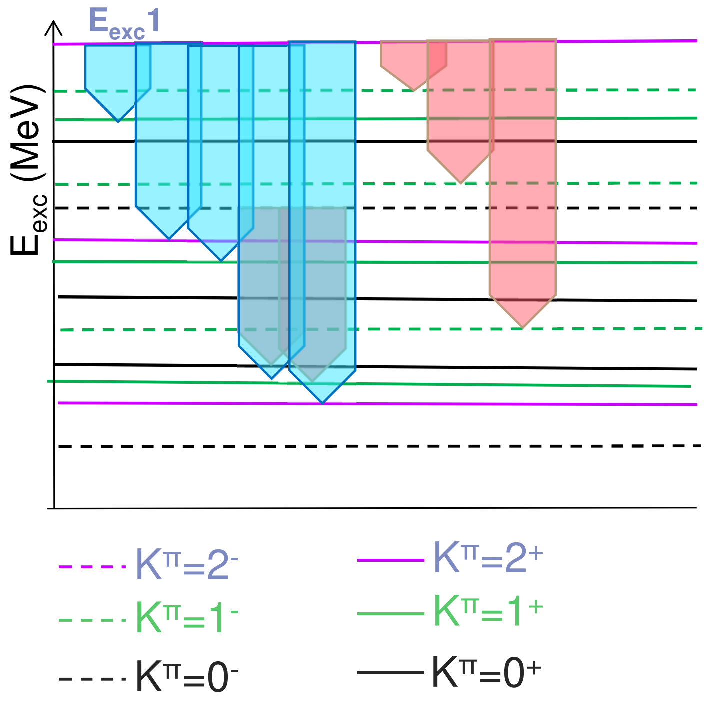

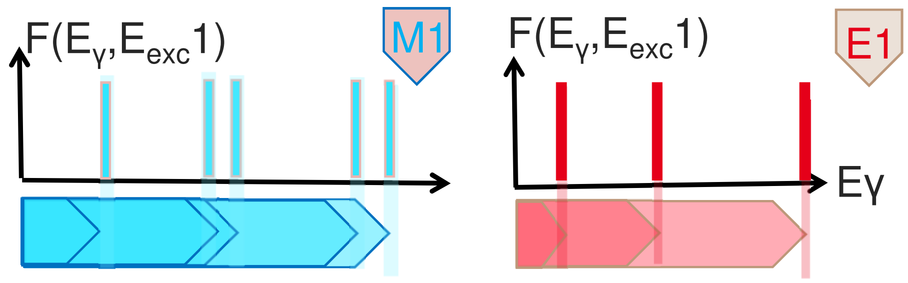

Absorption versus decay 2/2

The γ-ray strength function depends on the excitation energy and on the level density

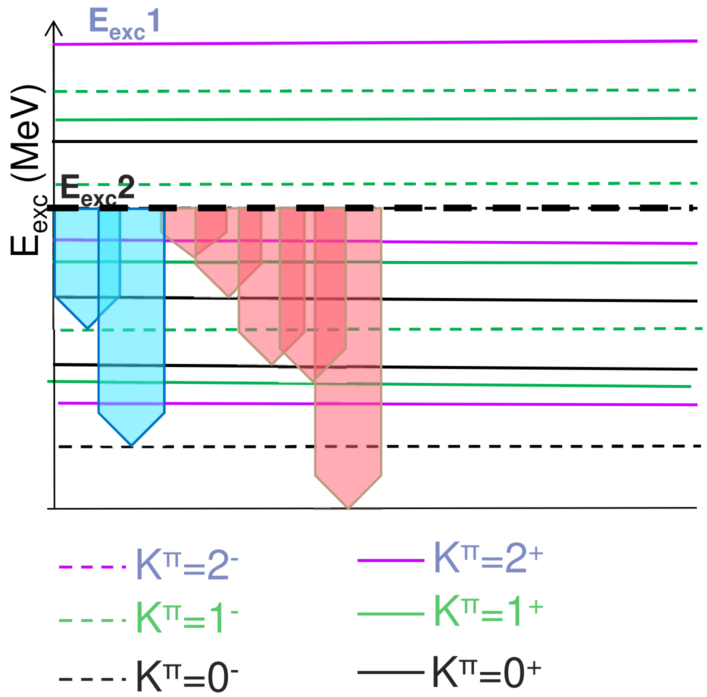

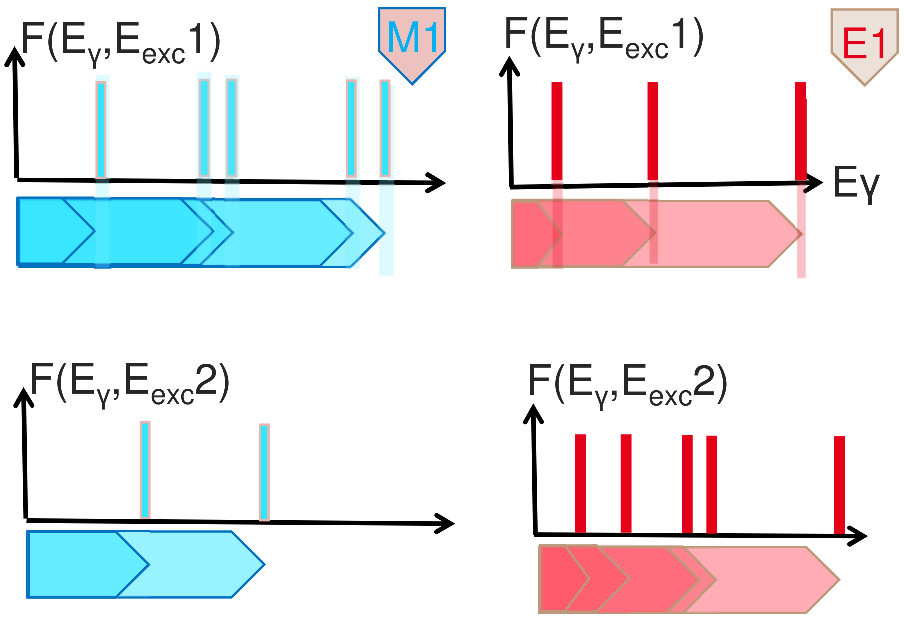

Absorption versus decay 2/2

The γ-ray strength function depends on the excitation energy and on the level density

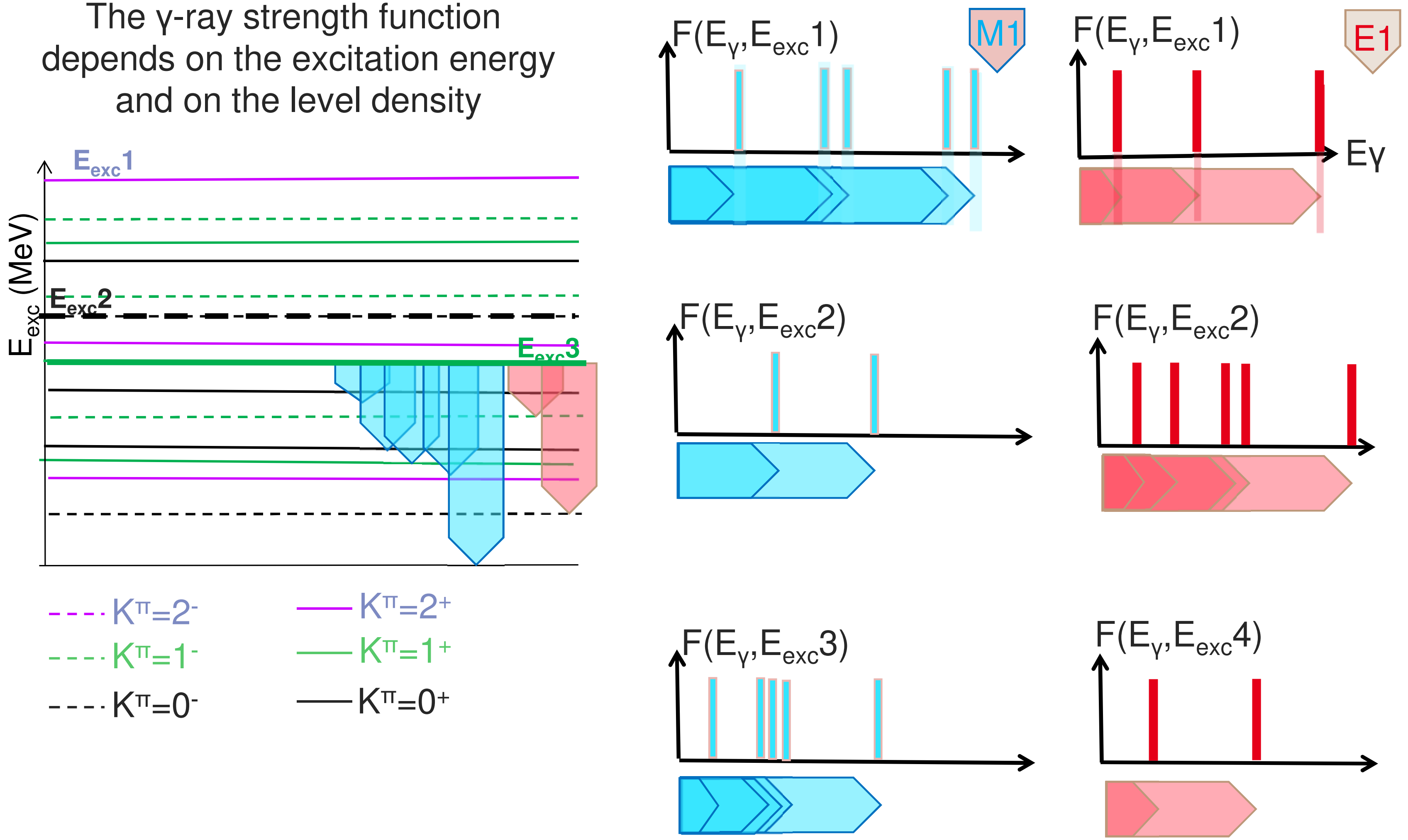

Absorption versus gamma decay, again…

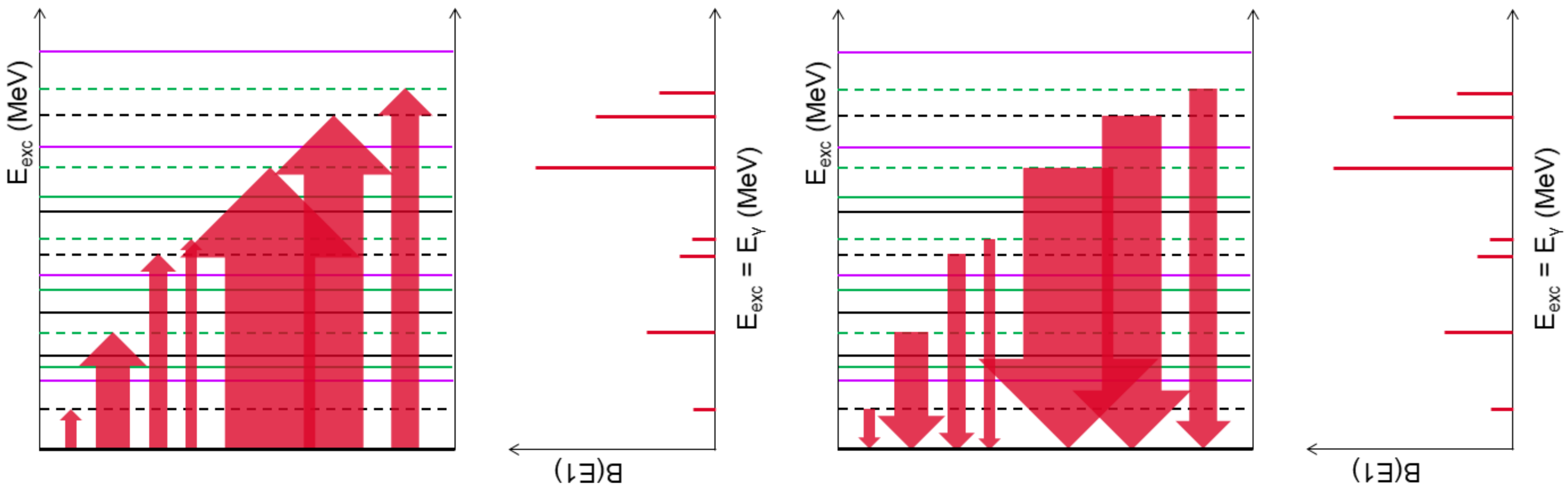

E emission γ = E excitation

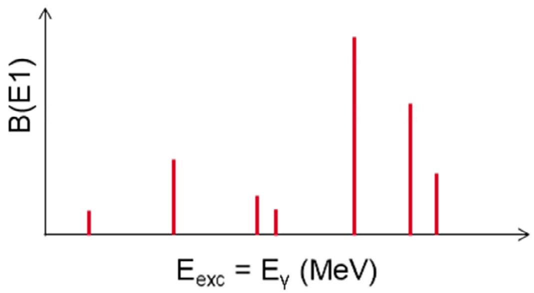

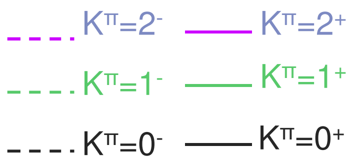

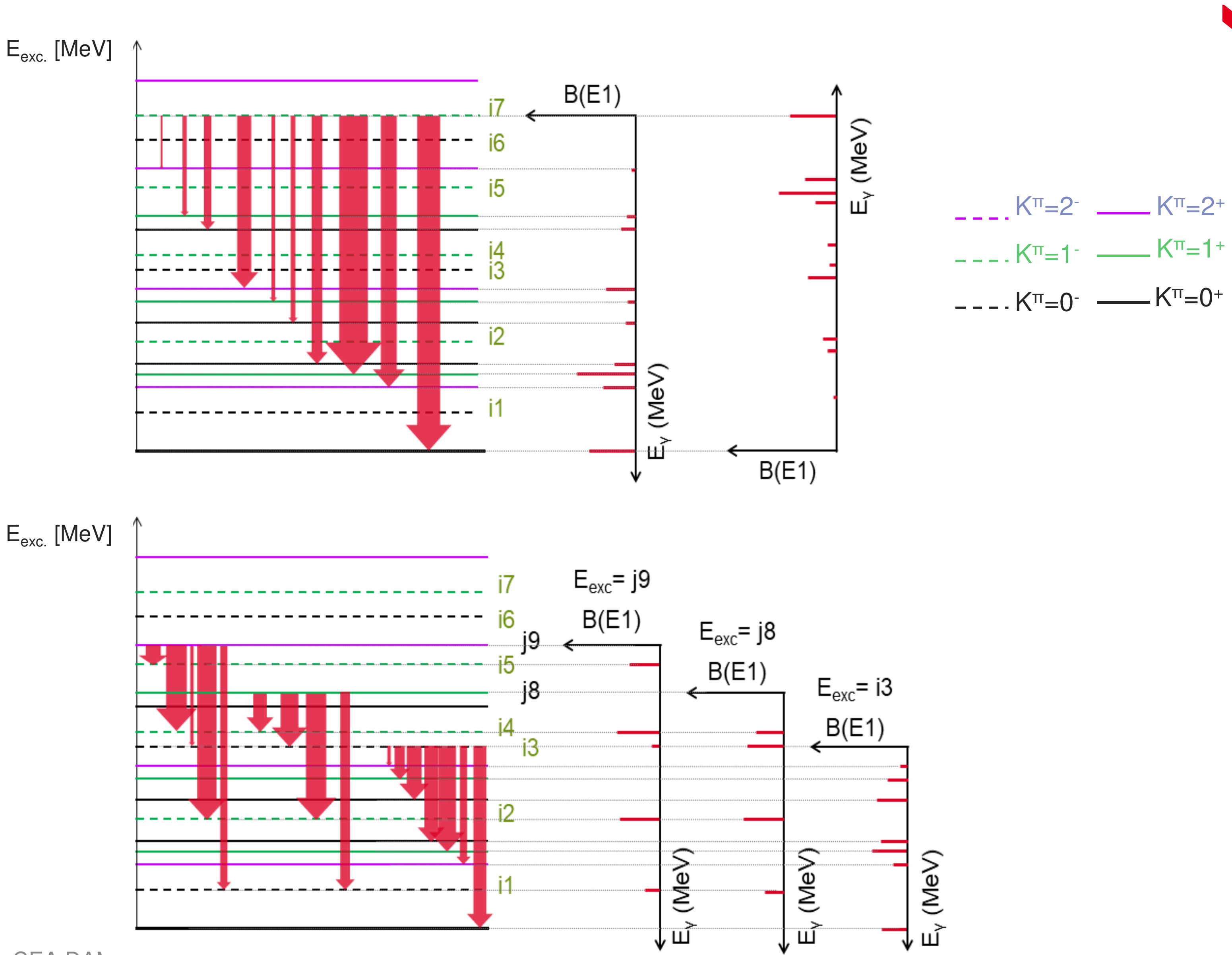

E exc. [MeV]
B(E1)
i7
i6
i5
i4
i3
i2
i1
Eγ (MeV)
B(E1)
Eγ (MeV)
Kπ=2-
Kπ=2+
Kπ=1-
Kπ=1+
Kπ=0-
Kπ=0+
E exc. [MeV]
E exc= j9
B(E1)
j9
E exc= j8
B(E1)
j8
E exc= i3
B(E1)
Eγ (MeV)
Eγ (MeV)
Eγ (MeV)

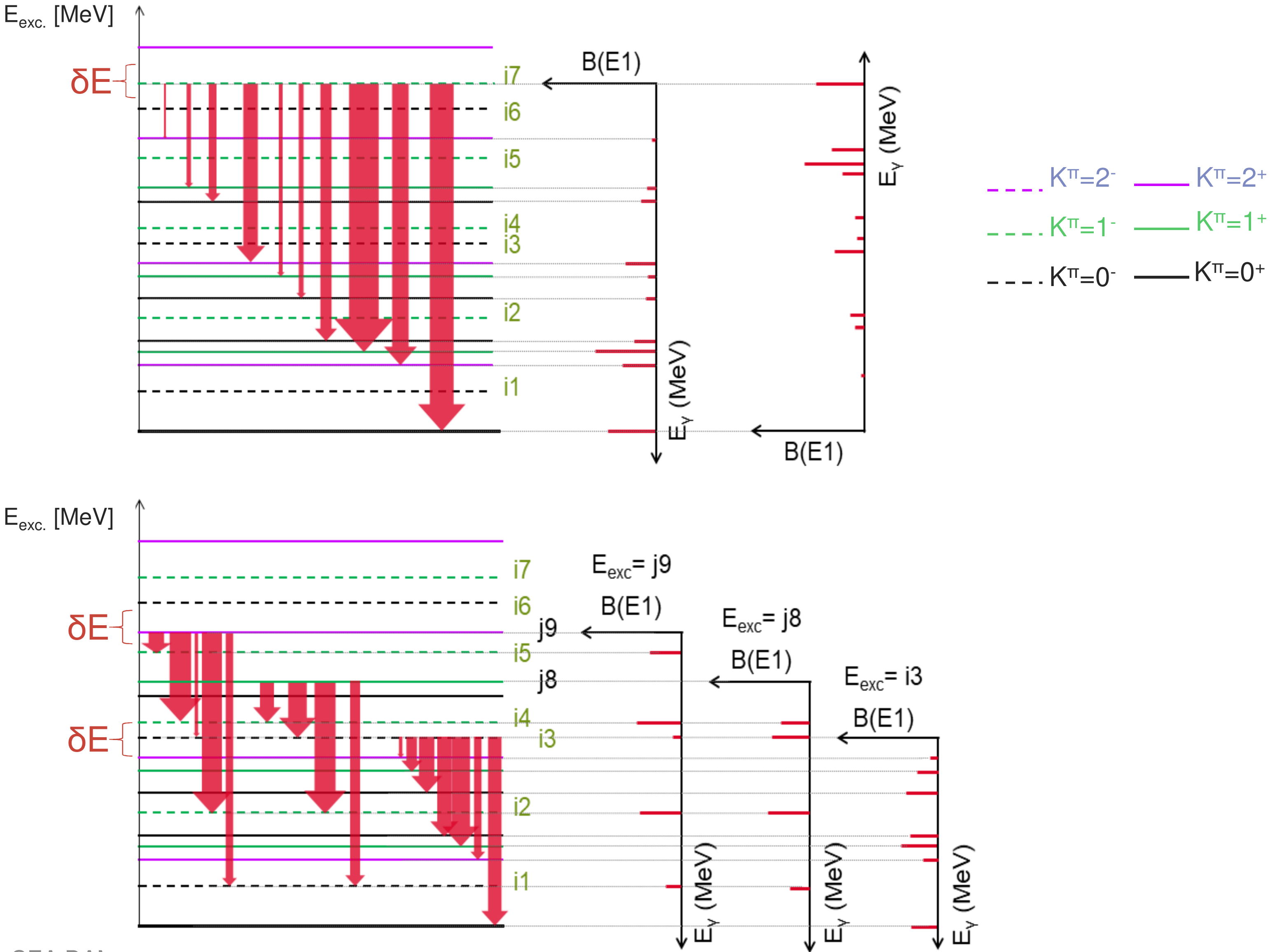

Eexc. [MeV]
δE
i7
i6
i5
i4
i3
i2
i1
B(E1)
Eγ (MeV)
B(E1)
Eγ (MeV)
Kπ=2-
Kπ=2+
Kπ=1-
Kπ=1+
Kπ=0-
Kπ=0+
Eexc. [MeV]
δE
δE
i7
i6
j9
i5
j8
i4
i3
i2
i1
Eexc= j9
B(E1)
Eexc= j8
B(E1)
Eexc= i3
B(E1)
Eγ (MeV)
Eγ (MeV)
Eγ (MeV)

Rotational bands in deformed nuclei

$$E_J = E_K + E_{rot} \quad \text{with} \quad E_{rot} = \frac{J(J+1)-K^2}{2I_x(Z,N)}$$

E_{exc} ≈ Temperature

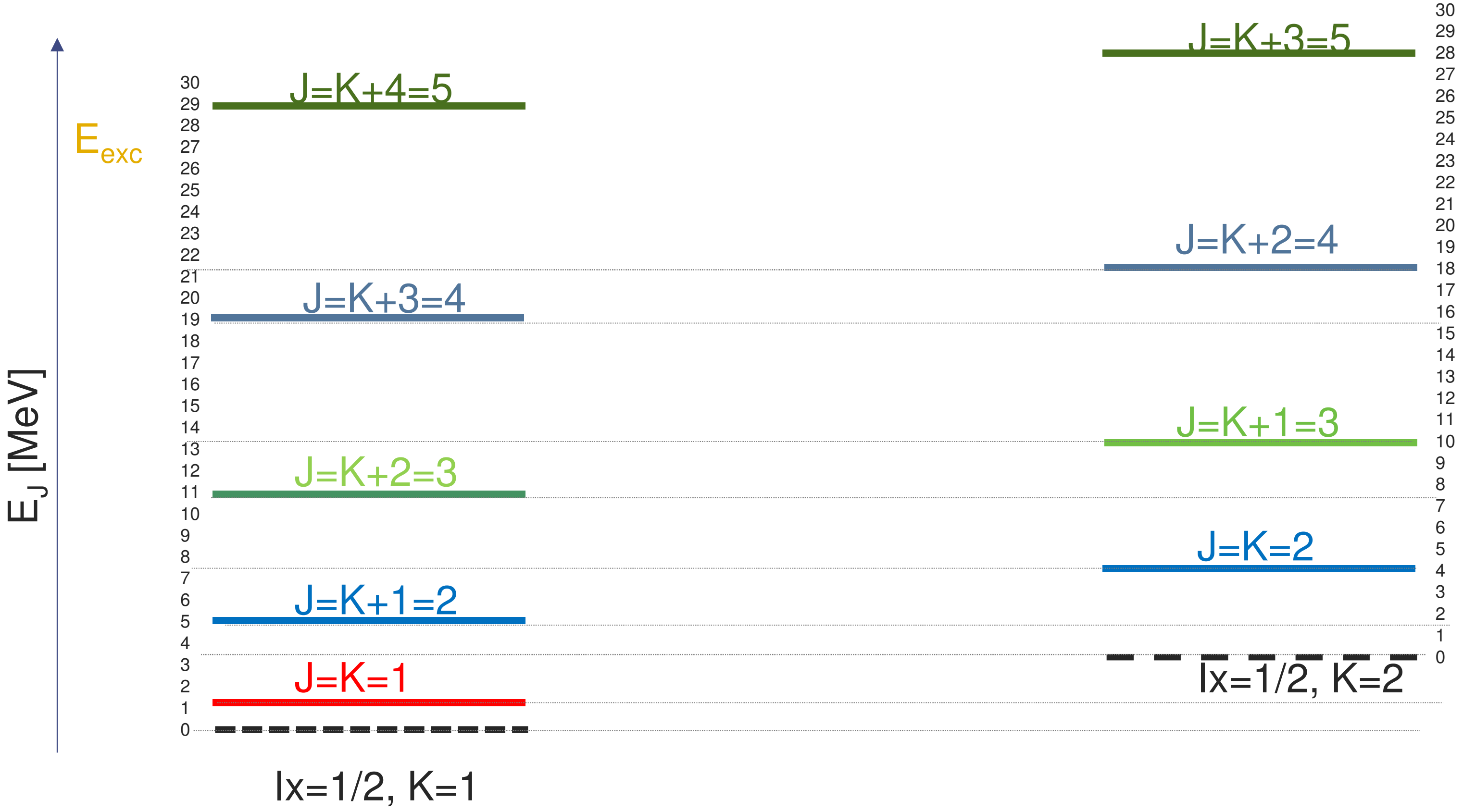

Gamma emission in deformed nuclei

Intra band transition probability calculations

Inter band transition probability calculations

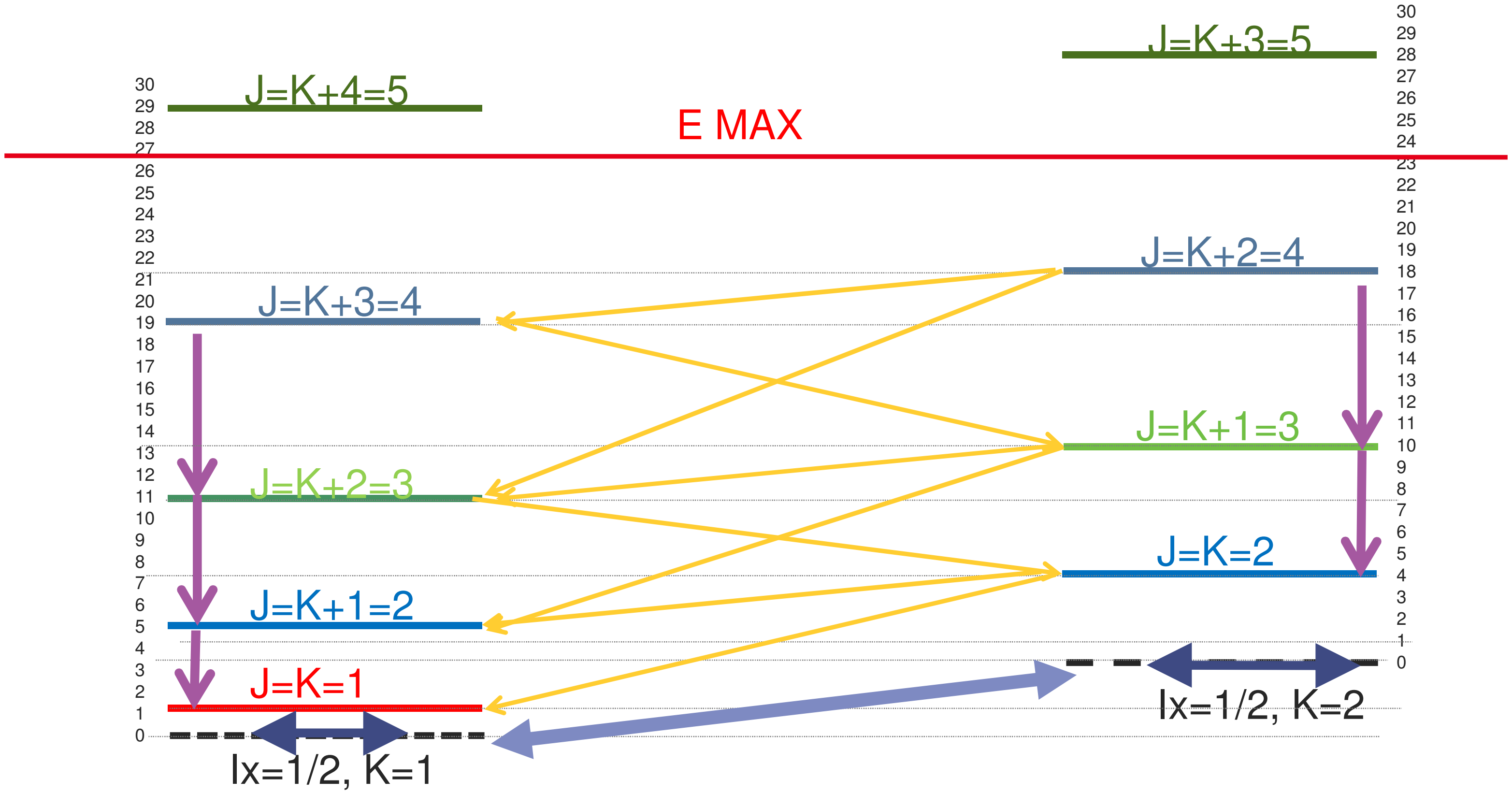

Gamma emission in deformed nuclei

Intra band transition probability calculations

Inter band transition probability calculations

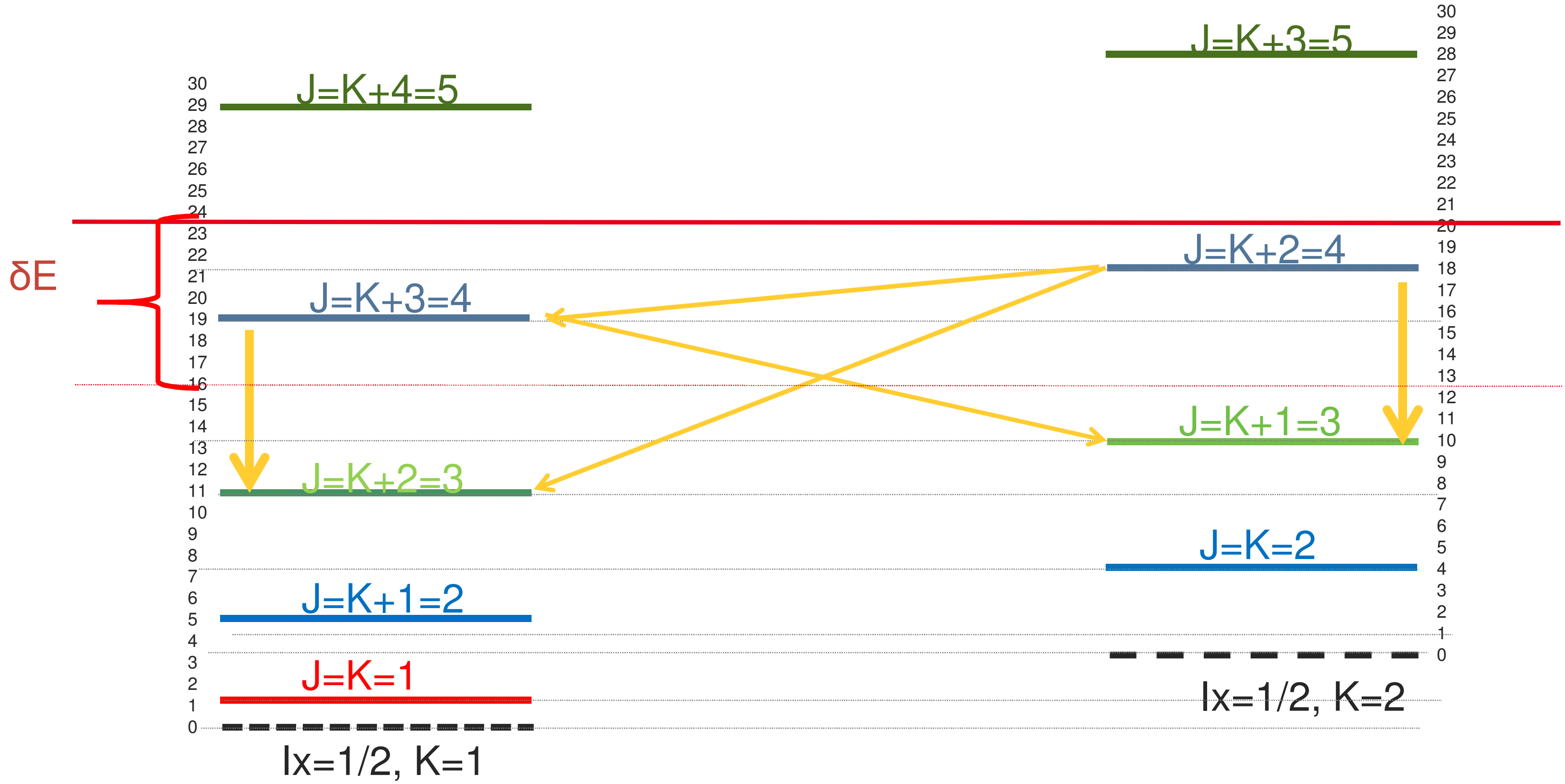

Gamma emission in deformed nuclei

Intra band transition probability calculations

Inter band transition probability calculations

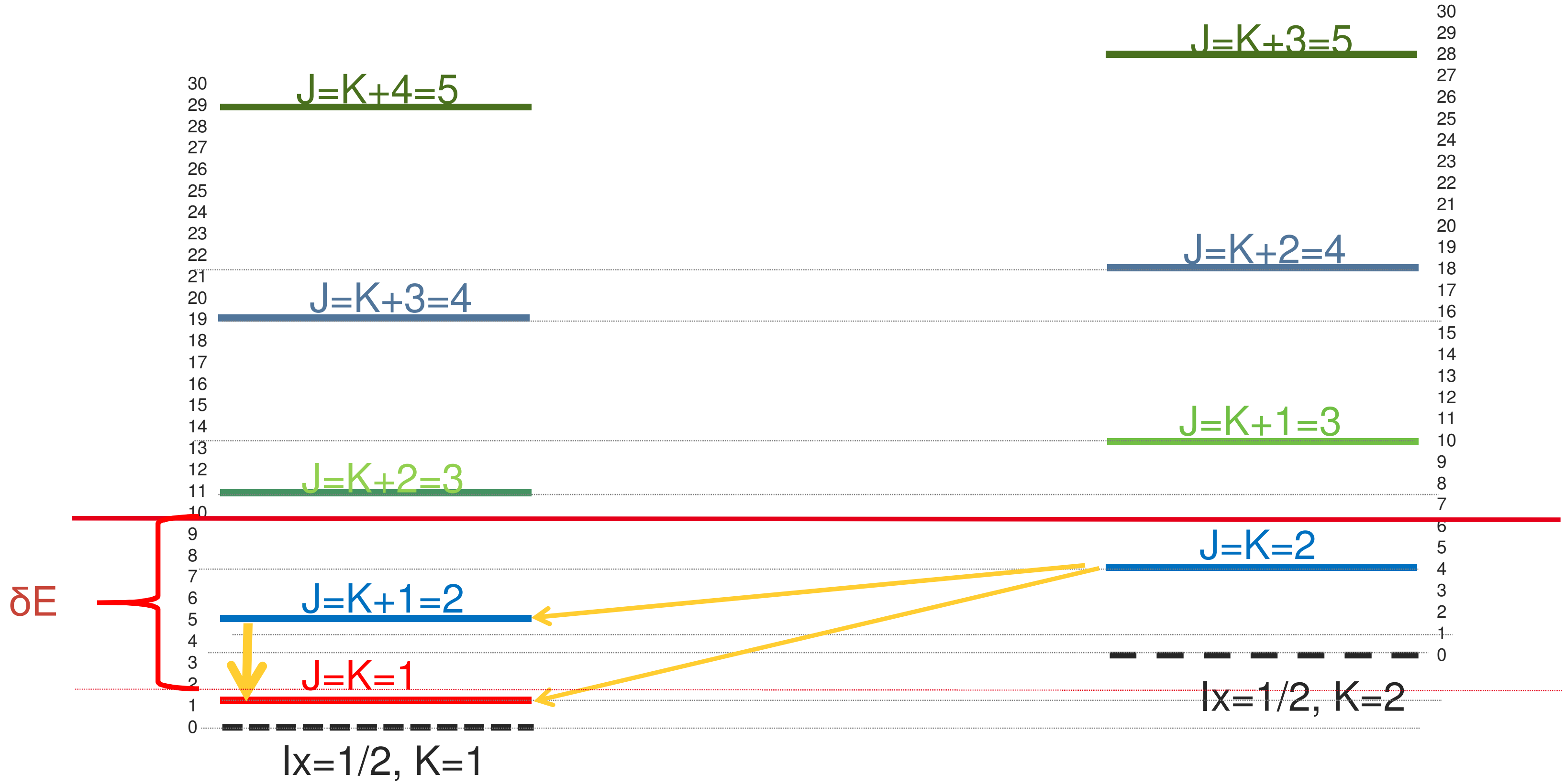

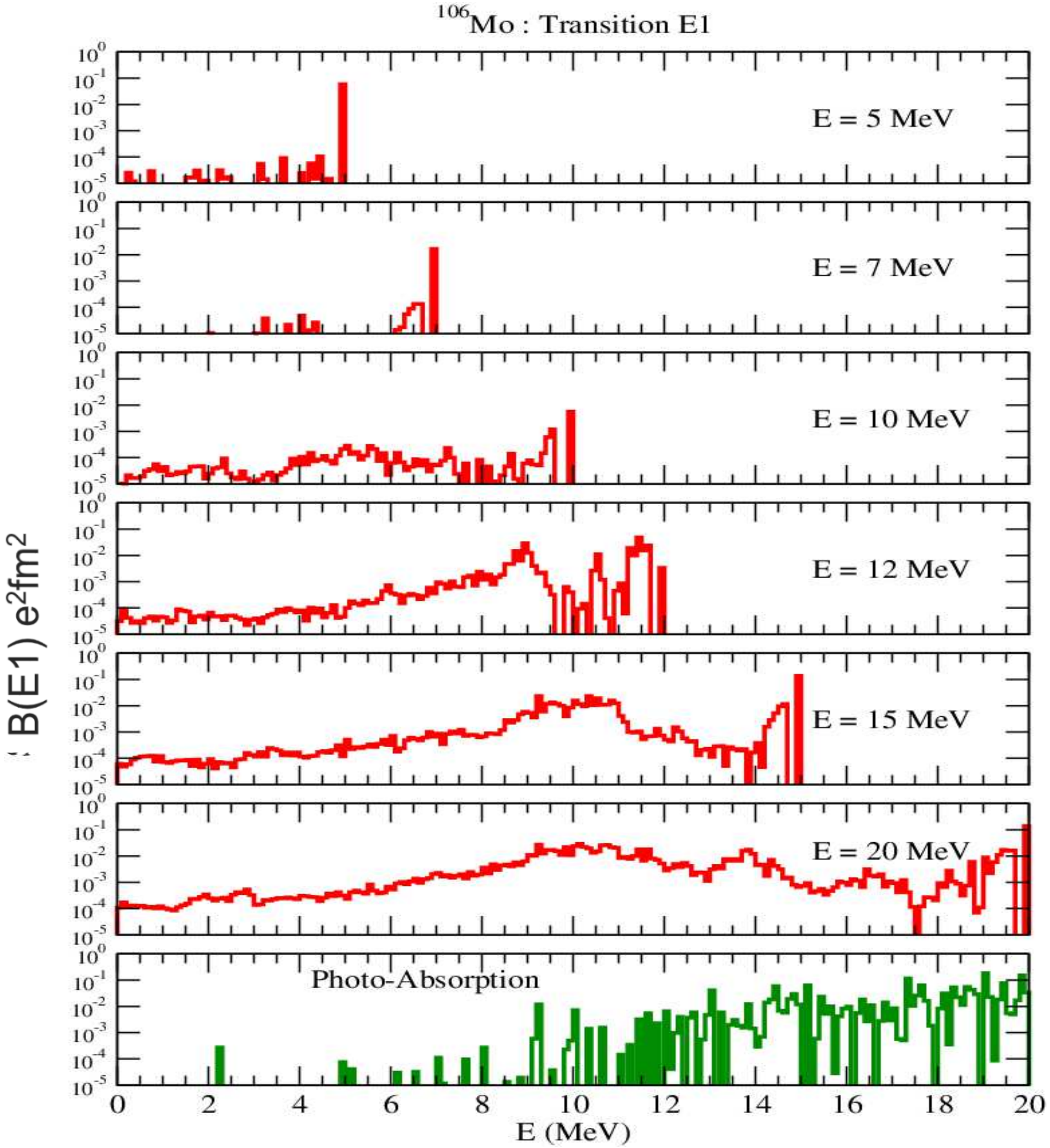
^{106}Mo : Transition E1
B(E1) e^2fm^2
E = 5 MeV
E = 7 MeV
E = 10 MeV
E = 12 MeV
E = 15 MeV
E = 20 MeV
Photo-Absorption
E (MeV)

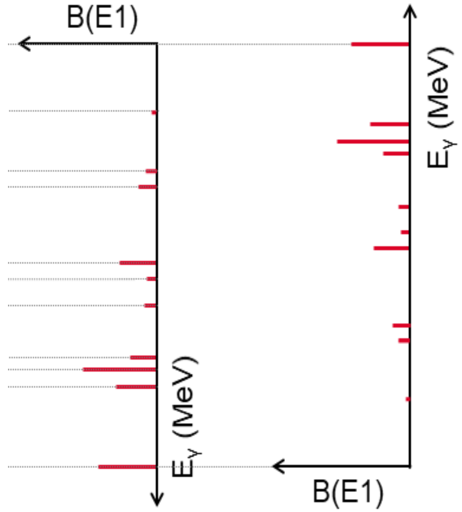
B(E1)
E_γ (MeV)
E_γ (MeV)
B(E1)

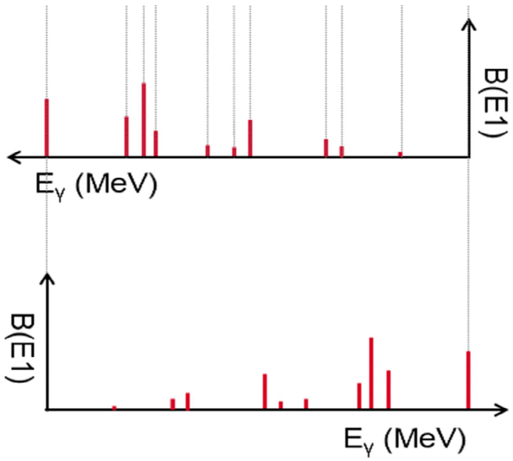
B(E1)
E_γ (MeV)
B(E1)
E_γ (MeV)

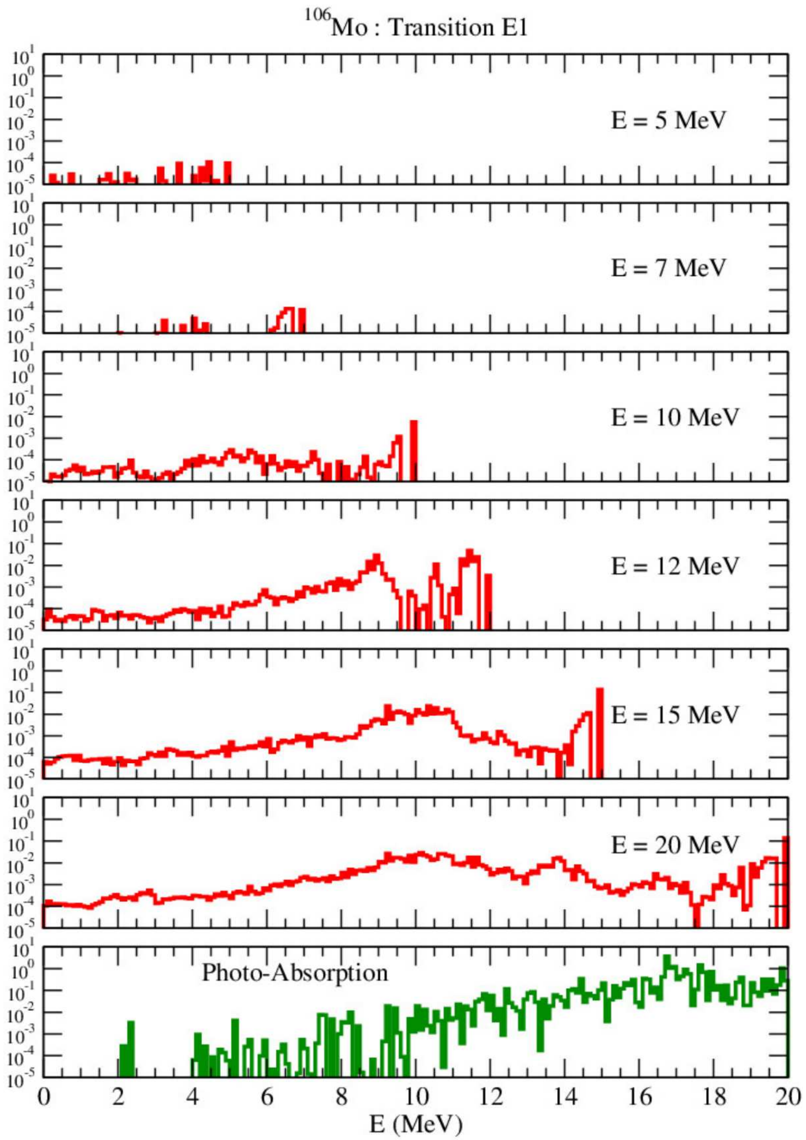

^{106}Mo : Transition E1
E = 5 MeV
E = 7 MeV
E = 10 MeV
E = 12 MeV
E = 15 MeV
E = 20 MeV
Photo-Absorption
E (MeV)

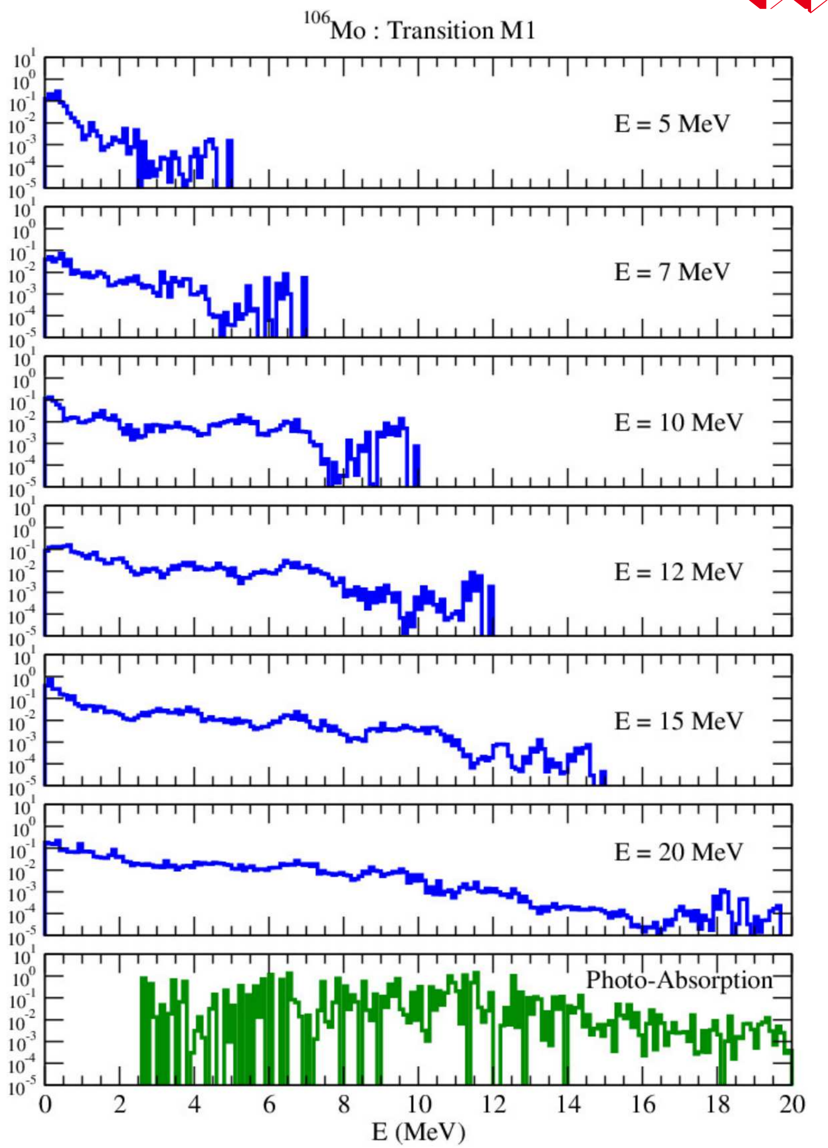

^{106}Mo : Transition M1
E = 5 MeV
E = 7 MeV
E = 10 MeV
E = 12 MeV
E = 15 MeV
E = 20 MeV
Photo-Absorption
E (MeV)

“ That’s all folks ! “